Localization Algorithms for Passive Sensor Networks

by

Darya Ismailova
B.Sc., University of Astrakhan, 2010

A Thesis Submitted in Partial Fulfillment of the
Requirements for the Degree of

MASTER OF APPLIED SCIENCE

in the Department of Electricanl and Computer Engineering

© Darya Ismailova, 2016
University of Victoria

All rights reserved. This dissertation may not be reproduced in whole or in part, by photocopying or other means, without the permission of the author.

Localization Algorithms for Passive Sensor Networks

by

Darya Ismailova
B.Sc., University of Astrakhan, 2010

Supervisory Committee

Dr. Wu-Sheng Lu, Supervisor
(Department of Electrical and Computer Engineering)

Dr. Pan Agathoklis, Departmental Member
(Department of Electrical and Computer Engineering)

Supervisory Committee

Dr. Wu-Sheng Lu, Supervisor
(Department of Electrical and Computer Engineering)

Dr. Pan Agathoklis, Departmental Member
(Department of Electrical and Computer Engineering)

ABSTRACT

...

Contents

List of Tables

List of Figures

ACKNOWLEDGEMENTS

Chapter 1

Introduction

1.1 My Claims

1.2 The Localization Problem

TODO

Review of ranging and localization methods, theory behind it, application, limitations.

TDOA,

AOA ?,

non-range-based?

"Geolocation techniques"

1.3 Contributions and Organization of the Thesis

1.3.1 Contributions of the Thesis

1.3.2 Organization of the Thesis

Chapter 2

Iterative Re-Weighting Least-Squares Methods for Source Localization

Locating a radiating source from range or range-difference measurements in a passive sensor network has recently attracted an increasing amount of research interest as it finds applications in a wide range of network-based wireless systems. Among the useful localization methods that have been documented over the years, least squares based algorithms constitute an important class of solution techniques as they are geometrically meaningful and often provide low complexity solution procedures with competitive estimation accuracy [1] - [15]. On the other hand, the error measure in a least squares (LS) formulation for the localization problem of interest is shown to be highly nonconvex, possessing multiple local solutions with degraded performance. There are many methods for continuous unconstrained optimization [33], however most of them are *local* methods that are sensitive to where the iteration begins, and give no guarantee to yield global solutions when applied to non-convex objective functions. In the case of source localization, this inherent feature of local methods is particular problematic because the source location is assumed to be entirely unknown and can appear practically anywhere, thus the chances to secure a good initial point for a local algorithm are next to none. For these reasons, various "global" localization techniques were investigated that are either non-iterative or insensitive to initial iterate. One representative in the class of global localization methods is the convex-relaxation based algorithm for range measurements proposed in [11], where

the least squares model is relaxed to a semidefinite programming problem which is known to be convex [32], hence robust to where it starts. Another representative in this class is reference [15], where localization problems for range as well as range difference measurements are addressed by developing solution methods for *squared* range LS (SR-LS) and *squared* range difference LS (SRD-LS) problems. The methods proposed in [15] are non-iterative and the solutions obtained are proven to be the global minimizers of the respective SR-LS and SRD-LS problems, which are shown to be excellent estimates of the original LS solutions.

This chapter presents improved least squares methods that demonstrate improved localization performance when compared with some best known results from the literature. The key new ingredient of the proposed algorithms is an iterative procedure where the SR-LS (SRD-LS) algorithm is iteratively applied to a weighted sum of squared terms where the weights are carefully designed so that the iterates produced quickly converge to a solution which is found to be considerably closer to the original range-based (range-difference-based) LS solution.

2.1 Source Localization From Range Measurements

2.1.1 Problem Statement

The source localization problem considered here involves a given array of m sensors specified by $\{\boldsymbol{a}_1, \ldots, \boldsymbol{a}_m\}$ where $\boldsymbol{a}_i \in R^n$ contains the n coordinates of the ith sensor in space R^n. Each sensor measures its distance to a radiating source $\boldsymbol{x} \in R^n$. Throughout it is assumed that only noisy copies of the distance data are available, hence the *range measurements* obey the model

$$r_i = \|\boldsymbol{x} - \boldsymbol{a}_i\| + \varepsilon_i, i = 1, \ldots, m. \tag{2.1}$$

where ε_i denotes the unknown noise that has occurred when the ith sensor measures its distance to source $\boldsymbol{x}$. Let $\boldsymbol{r} = [r_1\ r_2 \ldots r_m]^T$ and $\boldsymbol{\varepsilon} = [\varepsilon_1\ \varepsilon_2 \ldots \varepsilon_m]^T$. The source localization problem can be stated as to estimate the exact source location $\boldsymbol{x}$ from the noisy range measurements $\boldsymbol{r}$. In the rest of this section, a least-squares (LS) formulation of the localization problem and two most relevant state-of-the-art solution methods are briefly reviewed; and a new method based on iterative re-weighting of squared range LS technique as well as a variant of the proposed method are then

presented.

2.1.2 LS Formulations and Review of Related Work

Least squares approaches have proven effective for source localization problems [1] -[15]. For the localization problem at hand, the range-based least squares (R-LS) estimate refers to the solution of the problem

$$\underset{\boldsymbol{x}}{\text{minimize}}\, f(\boldsymbol{x}) \equiv \sum_{i=1}^{m} (r_i - \|\boldsymbol{x} - \boldsymbol{a}_i\|)^2 \tag{2.2}$$

The primary reason that justifies formulation (2.2) is its connection to the maximum-likelihood location estimation that determines $\boldsymbol{x}$ by examining the probabilistic model of the error vector $\boldsymbol{\varepsilon}$. Assuming the errors ε_i are independently and identically distributed (i.i.d) Gaussian variables with zero mean and variance σ_i^2, then $\boldsymbol{\varepsilon}$ obeys a Gaussian distribution with zero mean and covariance $\boldsymbol{\Sigma} = \text{diag}(\sigma_1^2, \ldots, \sigma_m^2)$, and the maximum likelihood (ML) location estimator in this case is known to be

$$\boldsymbol{x}_{ML} = \arg \min_{\boldsymbol{x} \in R^n} (\boldsymbol{r} - \boldsymbol{g})^T \Sigma^{-1} (\boldsymbol{r} - \boldsymbol{g}) \tag{2.3}$$

where $\boldsymbol{g} = [g_1\ g_2 \ldots\ g_m]^T$ with

$$g_i = \|\boldsymbol{x} - \boldsymbol{a}_i\| \tag{2.4}$$

It follows immediately that the ML solution in (2.3) is identical to the R-LS solution of problem (2.2) when covariance $\boldsymbol{\Sigma}$ is proportional to the identity matrix, i.e., $\sigma_1^2 = \ldots = \sigma_m^2$. In the literature this is known as the equal noise power case. For notation simplicity the method described in this chapter focuses on the equal noise power case, however the method developed below is also applicable to the unequal noise power case by working on a weighted version of the objective in (2.2) with $\{\sigma_i^{-2}, i = 1, \ldots, m\}$ as the weights.

Although many methods for unconstrained optimization are available [33], most of them are *local* methods in the sense they are sensitive to the choice of initial point where the iteration of an optimization algorithm begins. Especially when applied to a nonconvex objective function which possesses a number of local minimizers, unless a chosen local method starts at an initial point that happens to be sufficiently close to the (unknown) global minimizer, the solution obtained by the method gives no guaranty about global minimality. Unfortunately, the objective in (2.2) is highly

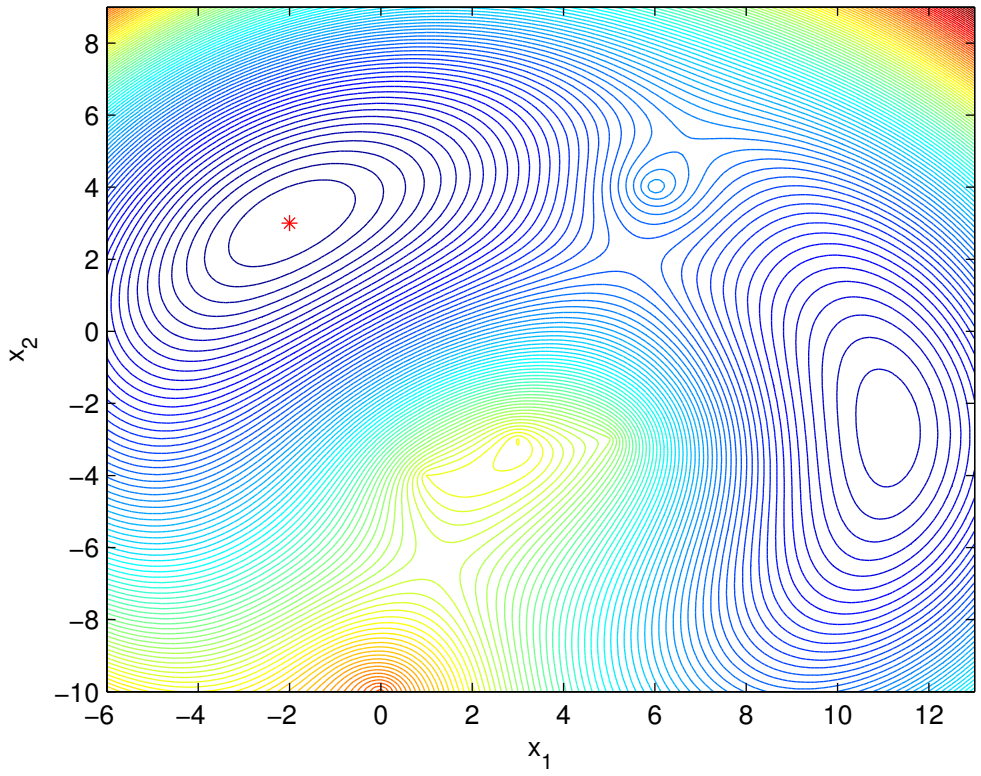

Figure 2.1: Contours of the R-LS objective function over the region $\Re = \{\boldsymbol{x} : -6 \leq x_1 \leq 13, -10 \leq x_2 \leq 9\}$

nonconvex, possessing many local minimizers even for small-scale systems. As an example, consider an instance of the source localization problem on the plane $n = 2$ with five sensors $m = 5$ located at $(6, 4)^T, (0, -10)^T, (5, -3)^T, (1, -4)^T$ and $(3, -3)^T$ with the source emmitting the signal at $\boldsymbol{x}_s = (-2, 3)^T$. Figure 2.1 describes a contour plot of the R-LS objective function in (2.2) over the region $\Re = \{\boldsymbol{x} : -6 \leq x_1 \leq 13, -10 \leq x_2 \leq 9\}$. It can be observed from the plot that there are two minimizers at $\tilde{\boldsymbol{x}} = (-1.9907, 3.0474)^T$ and $\widehat{\boldsymbol{x}} = (11.1152, -2.6785)^T$ with values of the objective $f(\tilde{\boldsymbol{x}}) = 0.1048$ and $f(\widehat{\boldsymbol{x}}) = 15.0083$ respectively. As expected, the global minimizer of R-LS objective offers a good approximation of the exact source location $\boldsymbol{x}_s$, but is unlikely to be precisely at point $\boldsymbol{x}_s$ because the objective $f(\boldsymbol{x})$ is defined using noisy range measurements. Note that for the exact source location $\boldsymbol{x}_s$ we have $f(\boldsymbol{x}_s) = \sum_{i=1}^{m} \varepsilon_i^2$.

Reference [11] addresses problem (2.2) by a convex relaxation technique where (2.2) is modified to a convex problem known as semidefinite programming (SDP)

[32]. A key step in this procedure is to use (2.4) with g_i as new variables, which leads (2.2) to the constrained problem

$$\underset{\boldsymbol{x},\boldsymbol{g}}{\text{minimize}} \sum_{i=1}^{m} (r_i - g_i)^2 \tag{2.5a}$$

$$\text{subject to:} \quad g_i^2 = \|\boldsymbol{x} - \boldsymbol{a}_i\|^2, \quad i = 1, \ldots, m. \tag{2.5b}$$

By further defining matrix variables

$$\boldsymbol{G} = \begin{bmatrix} \boldsymbol{g} \\ 1 \end{bmatrix} \begin{bmatrix} \boldsymbol{g}^T & 1 \end{bmatrix} \text{ and } \boldsymbol{X} = \begin{bmatrix} \boldsymbol{x} \\ 1 \end{bmatrix} \begin{bmatrix} \boldsymbol{x}^T & 1 \end{bmatrix} \tag{2.6}$$

and neglecting the rank constrains on $\boldsymbol{G}$ and $\boldsymbol{X}$, (2.5) can be reformulated in term of variables $\boldsymbol{G}$ and $\boldsymbol{X}$ as

$$\underset{\boldsymbol{X},\boldsymbol{G}}{\text{minimize}} \sum_{i=1}^{m} \left(G_{ii} - 2r_i G_{m+1,i} + r_i^2 \right) \tag{2.7a}$$

$$\text{subject to:} \quad G_{ii} = Tr\left(\boldsymbol{C}_i \boldsymbol{X}\right), i = 1, \ldots, m \tag{2.7b}$$

$$\boldsymbol{G} \succeq 0, \boldsymbol{X} \succeq 0 \tag{2.7c}$$

$$G_{m+1,m+1} = G_{n+1,n+1} = 1 \tag{2.7d}$$

where

$$C_i = \begin{pmatrix} \boldsymbol{I}_{n\times n} & -\boldsymbol{a}_i \\ -\boldsymbol{a}_i^T & \|\boldsymbol{a}_i\|^2 \end{pmatrix} \quad i = 1, \ldots, m \tag{2.8}$$

which is a standard SDP problem that can be solved efficiently [32, 33]. Note that because (2.7) is a convex problem, global minimality of the solution is ensured regardless of the initial point used. On the other hand, however, because (2.7) is an approximation of the original problem in (2.2), the solution of (2.7) is only an approximate solution of problem (2.2). In what follows the solutions obtained by this SDP-relaxation based method will be referred to as SDR-LS solutions.

A rather different approach is recently proposed in [15] where the localization problem (2.2) is tackled by developing techniques that find global solution of the *squared range based LS* (SR-LS) problem

$$\underset{\boldsymbol{x}}{\text{minimize}} \sum_{i=1}^{m} \left(\|\boldsymbol{x} - \boldsymbol{a}_i\|^2 - r_i^2 \right)^2 \tag{2.9}$$

By writing the objective in (2.9) as $\left(\alpha - 2\boldsymbol{a}_i^T\boldsymbol{x} + \|\boldsymbol{a}_i\|^2 - r_i^2\right)^2$ with $\alpha = \|\boldsymbol{x}\|^2$, it becomes a convex quadratic objective if one treats α as an additional variable and $\alpha = \|\boldsymbol{x}\|^2$ as a constraint. In this way, (2.9) is converted to the following constrained LS problem after necessary variable changes:

$$\underset{\boldsymbol{y}\in R^{n+1}}{\text{minimize}}\, \|\boldsymbol{A}\boldsymbol{y} - \boldsymbol{b}\|^2 \tag{2.10a}$$

$$\text{subject to:}\quad \boldsymbol{y}^T\boldsymbol{D}\boldsymbol{y} + 2\boldsymbol{f}^T\boldsymbol{y} = 0 \tag{2.10b}$$

where and

$$\boldsymbol{y} = \begin{pmatrix} \boldsymbol{x} \\ \|\boldsymbol{x}\|^2 \end{pmatrix},\ \boldsymbol{A} = \begin{pmatrix} -2\boldsymbol{a}_1^T & 1 \\ \vdots & \vdots \\ -2\boldsymbol{a}_m^T & 1 \end{pmatrix},\ \boldsymbol{b} = \begin{pmatrix} r_1^2 - \|\boldsymbol{a}_1\|^2 \\ \vdots \\ r_m^2 - \|\boldsymbol{a}_m\|^2 \end{pmatrix} \tag{2.11}$$

$$\boldsymbol{D} = \begin{pmatrix} \boldsymbol{I}_{n\times n} & \boldsymbol{0}_{n\times n} \\ \boldsymbol{0}_{n\times n} & 0 \end{pmatrix},\ \boldsymbol{f} = \begin{pmatrix} \boldsymbol{0} \\ -0.5 \end{pmatrix}$$

This problem conversion, made in [15], turns out to be crucial as problem (2.10), which remains to be nonconvex because of the nonlinear equality constraint (2.10b), falls into the class of generalized trust region subproblems (GTRS) [20, 21] whose global solutions can be computed by exploring the KKT conditions which are both necessary and sufficient optimality conditions in this case [20].

We now conclude this section with a couple of remarks. First, an unconstrained version of (2.10) may be obtained by neglecting the constraint in (2.10b) as

$$\underset{\boldsymbol{y}\in R^{n+1}}{\text{minimize}}\, \|\boldsymbol{A}\boldsymbol{y} - \boldsymbol{b}\|^2 \tag{2.12}$$

whose solution, called *unconstrained squared-range-based LS* (USR-LS) estimate, is given by

$$\boldsymbol{y}^* = \left(\boldsymbol{A}^T\boldsymbol{A}\right)^{-1}\boldsymbol{A}^T\boldsymbol{b} \tag{2.13}$$

It is demonstrated by numerical experiments [15] that the SR-LS solution outperforms the USR-LS and, in many cases, SDR solutions. Second, the SR-LS solution, although it solves (2.9) exactly, lacks the statistical interpretation of the ML formulation. The SR-LS remains to be an approximate solution for the original problem in (2.2) and, as it was demonstrated by the numerical results in [16] and [18], provides less accurate

estimates of the true source location, than the LS estimate. The method, described in detail below, tries to reduce the gap between the two solutions.

2.1.3 An Iterative Re-Weighting Approach

Iterative re-weighting least squares method is a popular technique used for solving problems involving the sums of norms. The method has found many applications, such as in robust regression [22, 23], sparse recovery [17], but the most relevand application for the current case is for solving the Fermat-Weber location problem. The Fermat–Weber problem has a long history and has been extensively studied in the field of optimization and location theory [23]. This problem can be stated as: Given m points $\boldsymbol{a}_1, \boldsymbol{a}_2, \ldots, \boldsymbol{a}_m \in R^n$ called *anchors* and nonnegative weights $\omega_1, \omega_2, \ldots, \omega_m > 0$, find $\boldsymbol{x} \in R^n$ that minimizes the weighted sum of Euclidian distances between $\boldsymbol{x}$ and the m anchors:

$$\underset{\boldsymbol{x} \in R^n}{\text{minimize}} \sum_{i=1}^{m} \omega_i \|\boldsymbol{x} - \boldsymbol{a}_i\|.$$

Fermat–Weber problem is much easier to analyze and solve than the ML problem (2.2) because it is a well-structured nonsmooth convex minimization problem. The similarities between the Fermat–Weber problem and problem (2.2) have been noted and addressed in the literature [16] with a gradient method with a fixed step size, known as the standard fixed point (SFP) algorithm, to deal with problem (2.2). However, being a gradient method, likelihood for the SFP algorithm to converge to a local solution exists. Another method, also proposed in [16] and known as the the sequential weighted least squares algorithm (SWLS), is also an iterative method where each iteration involves solving a nonlinear least squares problem similar to (2.9). The SWLS method is found to be superior over SFP in terms of convergence rate and a wider region of convergence to the global minimum [16]. However, the possibility for SWLS to converge to a local minimum remains in certain sensor setup even if the initial point is constructed using a procedure developed specifically for SWLS. The method presented below takes an approach that is different those described above in the sense that it does not require an initial point and the solution produced is guranteed to converge to a *global* solution.

Weighted squared range based least squares formulation

We now consider the weighted squared range based least squares (WSR-LS) problem

$$\underset{\boldsymbol{x}}{\text{minimize}} \sum_{i=1}^{m} w_i \left(\|\boldsymbol{x} - \boldsymbol{a}_i\|^2 - r_i^2 \right)^2 \tag{2.14}$$

which is obviously a weighted version of the SR-LS problem in (2.9). Following [15], it is rather straightforward to convert (2.14) into a GTRS similar to (2.10) as

$$\underset{\boldsymbol{y} \in R^{n+1}}{\text{minimize}} \, \|\boldsymbol{\Gamma} \left(\boldsymbol{A}\boldsymbol{y} - \boldsymbol{b} \right) \|^2 \tag{2.15a}$$

$$\text{subject to:} \quad \boldsymbol{y}^T \boldsymbol{D} \boldsymbol{y} + 2\boldsymbol{f}^T \boldsymbol{y} = 0 \tag{2.15b}$$

where $\boldsymbol{A}$, $\boldsymbol{b}$, $\boldsymbol{D}$, and $\boldsymbol{f}$ are defined in (2.11) and $\boldsymbol{\Gamma} = \text{diag}\left(\sqrt{w_1}, \ldots, \sqrt{w_m}\right)$. Clearly, problem (2.15) can be written as

$$\underset{\boldsymbol{y} \in R^{n+1}}{\text{minimize}} \, \|\boldsymbol{A}_w \boldsymbol{y} - \boldsymbol{b}_w\|^2 \tag{2.16a}$$

$$\text{subject to:} \quad \boldsymbol{y}^T \boldsymbol{D} \boldsymbol{y} + 2\boldsymbol{f}^T \boldsymbol{y} = 0 \tag{2.16b}$$

where $\boldsymbol{A}_w = \boldsymbol{\Gamma}\boldsymbol{A}$ and $\boldsymbol{b}_w = \boldsymbol{\Gamma}\boldsymbol{b}$. On comparing (2.16) with (2.10), if $S(\boldsymbol{A}, \boldsymbol{b}, \boldsymbol{D}, \boldsymbol{f})$ denotes a solver that produces the global solution of problem (2.10) for a given data set $\{\boldsymbol{A}, \boldsymbol{b}, \boldsymbol{D}, \boldsymbol{f}\}$, then the same solver produces the global solution of the weighted problem (2.14) as long as it is applied to the data set $\{\boldsymbol{A}_w, \boldsymbol{b}_w, \boldsymbol{D}, \boldsymbol{f}\}$. We stress that the weights $\{w_i, i = 1, \ldots, m\}$ in (2.14) are *fixed* nonnegative constants.

Moving the SR-LS solution towards R-LS solution via iterative re-weighting

The main idea here is to use the weights $\{w_i, i = 1, \ldots, m\}$ to tune the objective in (2.14) toward the objective in (2.2) so that the solution obtained by minimizing such a WSR-LS objective is expected to be closer toward that of the problem (2.2). To substantiate the idea, we compare the ith term of the objective in (2.14) with its counterpart in (2.2), namely,

$$\underbrace{w_i \left(\|\boldsymbol{x} - \boldsymbol{a}_i\|^2 - r_i^2 \right)^2}_{\text{in (15)}} \leftrightarrow \underbrace{\left(\|\boldsymbol{x} - \boldsymbol{a}_i\| - r_i \right)^2}_{\text{in (2)}} \tag{2.17}$$

and write the term in (2.14) as

$$w_i \left(\|\boldsymbol{x}-\boldsymbol{a}_i\|^2 - r_i^2\right)^2 = \\ w_i \left(\|\boldsymbol{x}-\boldsymbol{a}_i\| + r_i\right)^2 \underbrace{\left(\|\boldsymbol{x}-\boldsymbol{a}_i\| - r_i\right)^2}_{\text{same as in (2)}}$$

It follows that the objective in (2.14) would be the same as in (2.2) if the weights w_i were assigned to $1/\left(\|\boldsymbol{x}-\boldsymbol{a}_i\| + r_i\right)^2$. Evidently, weight assignments as such cannot be realized because w_i's must be fixed constants for (2.14) to be a globally solvable WSR-LS problem. A natural remedy to deal with this technical difficulty is to employ an iterative procedure whose kth iteration generates a global solution $\boldsymbol{x}_k$ of a WSR-LS sub-problem of the form

$$\underset{x}{\text{minimize}} \sum_{i=1}^{m} w_i^{(k)} \left(\|\boldsymbol{x}-\boldsymbol{a}_i\|^2 - r_i^2\right)^2 \tag{2.18}$$

where for $k \geq 2$ the weights $\{w_i^{(k)}, i = 1, \ldots, m\}$ are assigned using the previous iterate $\boldsymbol{x}_{k-1}$ as

$$w_i^{(k)} = \frac{1}{\left(\|\boldsymbol{x}_{k-1}-\boldsymbol{a}_i\| + r_i\right)^2} \tag{2.19}$$

while for $k = 1$ all weights $\{w_i^{(1)}, i = 1, \ldots, m\}$ are set to unity. Clearly the weights given by (2.19) are realizable. More importantly, when the iterates produced by solving (2.18) (namely $\boldsymbol{x}_k$ for $k = 1, 2, \ldots$) converge, in the kth iteration with k sufficiently large, the objective function of (2.18) in a small vicinity of its solution $\boldsymbol{x}_k$ is approximately equal to

$$\begin{aligned} &\sum_{i=1}^{m} w_i^{(k)} \left(\|\boldsymbol{x}-\boldsymbol{a}_i\|^2 - r_i^2\right)^2 \\ \approx &\sum_{i=1}^{m} w_i^{(k)} \left(\|\boldsymbol{x}_k-\boldsymbol{a}_i\|^2 - r_i^2\right)^2 \\ = &\sum_{i=1}^{m} w_i^{(k)} \left(\|\boldsymbol{x}_k-\boldsymbol{a}_i\| + r_i\right)^2 \left(\|\boldsymbol{x}_k-\boldsymbol{a}_i\| - r_i\right)^2 \\ \approx &\sum_{i=1}^{m} w_i^{(k)} \left(\|\boldsymbol{x}_{k-1}-\boldsymbol{a}_i\| + r_i\right)^2 \left(\|\boldsymbol{x}_k-\boldsymbol{a}_i\| - r_i\right)^2 \\ = &\sum_{i=1}^{m} \left(\|\boldsymbol{x}_k-\boldsymbol{a}_i\| - r_i\right)^2 \approx \sum_{i=1}^{m} \left(\|\boldsymbol{x}-\boldsymbol{a}_i\| - r_i\right)^2 \end{aligned}$$

In words, with the weights from (2.19), the limiting point of the iterates produced by iteratively solving WSR-LS problem (2.18) is expected to be close to the global solution of problem (2.2).

The algorithmic steps of the proposed localization method are outlined as follows.

Algorithm 1

1) Input data: Sensor locations $\{\boldsymbol{a}_i, i = 1, \ldots, m\}$, range measurements $\{r_i, i = 1, \ldots, m\}$, maximum number of iterations k_{max} and convergence tolerance ζ.

2) Generate data set $\{\boldsymbol{A}, \boldsymbol{b}, \boldsymbol{d}, \boldsymbol{f}\}$ as

$$\boldsymbol{A} = \begin{pmatrix} -2\boldsymbol{a}_1^T & 1 \\ \vdots & \vdots \\ -2\boldsymbol{a}_m^T & 1 \end{pmatrix}, \boldsymbol{b} = \begin{pmatrix} r_1^T - \|\boldsymbol{a}_1\|^T \\ \vdots \\ r_m^T - \|\boldsymbol{a}_m\|^T \end{pmatrix}$$

$$\boldsymbol{D} = \begin{pmatrix} \boldsymbol{I}_{n\times n} & \boldsymbol{0}_{n\times n} \\ \boldsymbol{0}_{n\times n} & 0 \end{pmatrix}, \boldsymbol{f} = \begin{pmatrix} \boldsymbol{0} \\ -0.5 \end{pmatrix}.$$

Set $k = 1, w_i^{(1)} = 1$ for $i = 1, \ldots, m$.

3) Set $\boldsymbol{\Gamma}_k = \text{diag}\left(\sqrt{w_1^{(k)}}, \ldots, \sqrt{w_m^{(k)}}\right)$, $\boldsymbol{A}_w = \boldsymbol{\Gamma}_k \boldsymbol{A}$ and $\boldsymbol{b}_w = \boldsymbol{\Gamma}_k \boldsymbol{b}$.

4) Solve the WSR-LS problem

$$\underset{x}{\text{minimize}} \sum_{i=1}^{m} w_i^{(k)} \left(\|\boldsymbol{x} - \boldsymbol{a}_i\|^2 - r_i^2\right)^2$$

by solving (2.16), i.e.

$$\underset{\boldsymbol{y}\in R^{n+1}}{\text{minimize}} \|\boldsymbol{A}_w \boldsymbol{y} - \boldsymbol{b}_w\|^2$$
$$\text{subject to: } \boldsymbol{y}^T \boldsymbol{D} \boldsymbol{y} + 2\boldsymbol{f}^T \boldsymbol{y} = 0$$

to obtain its global solution $\boldsymbol{x}_k$.

5) If $k = k_{max}$ or $\|\boldsymbol{x}_k - \boldsymbol{x}_{k-1}\| < \zeta$, terminate and output $\boldsymbol{x}_k$ as the solution; otherwise, set $k = k + 1$, update weights $\{w_i^{(k)}, i = 1, \ldots, m\}$ using

$$w_i^{(k)} = \frac{1}{\left(\|\boldsymbol{x}_{k-1} - \boldsymbol{a}_i\| + r_i\right)^2}$$

and repeat from Step 3).

From the steps in Algorithm 1, it follows that the complexity of the algorithm is practically equal to the complexity of the WSR-LS solver involved in Step 4 times the number of iterations, k. Computer simulations have indicated that the algorithm converges with a small number of iterations, typically a $k \leq 6$ suffices. For simplicity, the solutions obtained from Algorithm 1 are called IRWSR-LS solutions. Technical details on how to solve (2.16) can be found in Appendix 1.

A variant of Algorithm 1

As argued above, the IRWSR-LS solution from Algorithm 1 is expected to be an improved approximation of the global solution of R-LS problem in (2.2). However a small gap between the two solutions is inevitable owing to the approximate nature of the re-weighting strategy. In what follows we present a variant of Algorithm 1 that closes this gap by taking the IRWSR-LS solution as an initial point to run a good local unconstrained optimization algorithm for problem (2.2). The rationale behind this two-step approach is that the initial point produced in the first step by Algorithm 1 is highly likely within a sufficiently small vicinity of the exact global solution of problem (2.2), hence a good local method will lead it to the exact solution in a small number of iterations. We remark that such a "hybrid" approach is also expected to work with other "global" methods including the SDR-LS and SR-LS methods, but with a difference that employing an IRWSR-LS solution in the first step improves the closeness of the initial point, hence increases the likelihood of securing the exact global solution of problem (2.2) by a local method in the second step.

For the localization problem in question, the well-known Newton algorithm [33] is chosen as a local method because of its fast convergence and low complexity. We note that, unlike in a general scenario where the Newton algorithm is often considered numerically expensive because it requires to compute the inverse of the Hessian matrix, computing such an inverse is not costly in the present case because the dimension of the unknown vector $\boldsymbol{x}$ is extremely low: $n = 2$ or 3. Moreover, the Hessian matrix involved can be efficiently evaluated by a closed-form formula, as shown below.

To evaluate the Hessian of the objective $f(\boldsymbol{x})$ in (2.2), we assume $\boldsymbol{x} \neq \boldsymbol{a}_i$ for $i = 1, \ldots, m$, so that $f(\boldsymbol{x})$ is a smooth function of $\boldsymbol{x}$. The assumption simply means that the radiating source is away from the sensor at least by a certain distance, which appears to be reasonable for a practical localization problem. Under this

circumstance, the gradient and Hessian of $f(\boldsymbol{x})$ are found to be

$$\boldsymbol{g}(\boldsymbol{x}) = \sum_{i=1}^{m} \left(1 - \frac{r_i}{\|\boldsymbol{x} - \boldsymbol{a}_i\|})\right) (\boldsymbol{x} - \boldsymbol{a}_i) \tag{2.20a}$$

and

$$\boldsymbol{H}(\boldsymbol{x}) = 2\left(\tau \boldsymbol{I} + \boldsymbol{H}_1(\boldsymbol{x})\right) \tag{2.20b}$$

respectively, where

$$\tau = m - \sum_{i=1}^{m} \frac{r_i}{\|\boldsymbol{x} - \boldsymbol{a}_i\|}$$

and

$$\boldsymbol{H}_1(\boldsymbol{x}) = \sum_{i=1}^{m} \frac{r_i (\boldsymbol{x} - \boldsymbol{a}_i)(\boldsymbol{x} - \boldsymbol{a}_i)^T}{\|\boldsymbol{x} - \boldsymbol{a}_i\|^3}.$$

To ensure a descent Newton step, the positive definiteness of the Hessian $\boldsymbol{H}(\boldsymbol{x})$ needs to be examined and, in case $\boldsymbol{H}(\boldsymbol{x})$ is not positive definite, to be modified to guatrantee its positive definiteness. To this end, the eigen-decomposition of $\boldsymbol{H}(\boldsymbol{x})$, namely,

$$\boldsymbol{H}(\boldsymbol{x}) = \boldsymbol{U}\boldsymbol{\Lambda}\boldsymbol{U}^T$$

may be performed, where $\boldsymbol{U}$ is orthogonal and $\boldsymbol{\Lambda} = \text{diag}\left(\tau + \ \lambda_1, \ldots, \tau + \lambda_n\right)$ with $\{\lambda_i, i = 1, \ldots, n\}$ being eigenvalues of $\boldsymbol{H}_1(\boldsymbol{x})$. Let l_{min} be the smallest eigenvalue of $\boldsymbol{H}(\boldsymbol{x})$, namely $l_{min} = \min\left(\tau + \lambda_1, \ldots, \tau + \lambda_n\right)$. If $l_{min} > 0$, then $\boldsymbol{H}(\boldsymbol{x})$ is positive definite and the Newton algorithm is carried out without modification; if $l_{min} \leq 0$, then the algorithm uses a slightly modified Hessian given by

$$\tilde{\boldsymbol{H}}(\boldsymbol{x}) = \boldsymbol{U}\tilde{\boldsymbol{\Lambda}}\boldsymbol{U}^T$$

where $\tilde{\boldsymbol{\Lambda}} = \text{diag}\left(\tilde{\lambda}_1, \ldots, \tilde{\lambda}_n\right)$

$$\tilde{\lambda}_i = \begin{cases} \tau + \lambda_i & \text{if } \tau + \lambda_i > 0 \\ \delta & \text{if } \tau + \lambda_i \leq 0 \quad i = 1, \ldots, m \end{cases}$$

and δ a small positive constant. Obviously, $\tilde{\boldsymbol{H}}(\boldsymbol{x})$ is guaranteed to be positive definite. The search direction in the kth iteration of the modified Newton algorithm is given by

$$\boldsymbol{d}_k = -\boldsymbol{U}\tilde{\boldsymbol{\Lambda}}^{-1}\boldsymbol{U}^T g(\boldsymbol{x}_k)$$

where $g(\boldsymbol{x}_k)$ is given by (2.20). In what follows, solutions obtained by the proposed two-step method are called *hybrid* IRWSR-LS solutions.

2.1.4 Numerical Results

Performance of the proposed algorithms was evaluated and compared with existing state-of-the-art methods by Monte Carlo simulations with a set-up similar to that of [15]. SR-LS and SRD-LS solutions were used as performance benchmarks for Algorithm 1 and its variant. In both cases the system consisted of m sensors $\{\boldsymbol{a}_i, i = 1, 2, \ldots, m\}$ randomly placed in the planar region in R^2, and a radiating source $\boldsymbol{x}_s$, located randomly in the region R=$\{\boldsymbol{x} : (x_1, x_2)^T, -10 \leq x_1, x_2 \leq 10\}$. Coordinates of the source and sensors were generated for each dimension following a uniform distribution. Measurement noise $\{\varepsilon_i, i = 1, \ldots, m\}$ was modelled as i.i.d. Gaussian random variables with zero mean and variance σ^2. Accuracy of source location estimation was evaluated as the average of the squared position error $\|\boldsymbol{x}^* - \boldsymbol{x}_s\|^2$ where $\boldsymbol{x}_s$ denotes the exact source location and $\boldsymbol{x}^*$ is its estimation obtained by SR-LS, IRWSR-LS and hybrid-IRWSR-LS methods, respectively. Table 2.1 provides comparisons of these methods with SR-LS, where each table entry is a MSE averaged over 1,000 Monte Carlo runs of a given method for a given noise level. For the columns representing performance of the IRWSR-LS and *hybrid* IRWSR-LS methods each table entry lists their MSE and relative improvement over SR-LS solutions in percentage, in the format: MSE(% Improvement).

Table 2.1: MSE of position estimation for SR-LS, IRWSR-LS and *hybrid* IRWSR-LS methods

σ	SR - LS	IRWSR-LS (Im.,%)	*hybrid* IRWSR-LS (Im.,%)
1e-03	2.0325e-06	1.1996e-06 (41)	1.1994e-06 (41)
1e-02	1.8372e-04	1.2480e-04 (32)	1.2481e-04 (32)
1e-01	1.8361e-02	1.2223e-02 (33)	1.2214e-02 (33)
1e+0	2.3752e+00	1.5108e+00 (36)	1.5330e+00 (35)

Employing a set-up similar to that in [15], the simulation studies of Algorithm 1 and its variant considered $m = 5$ sensors placed in the region $[-15; 15] \times [-15; 15]$, with σ being one of four possible levels $\{10^{-3}, 10^{-2}, 10^{-1}, 1\}$. The range measurements

$\{r_i, i = 1, 2, \ldots, 5\}$ were calculated using (2.1) and Step 4 of Algorithm 1 was implemented using the SR-LS algorithm proposed in [15]. It is observed that IRWSR-LS solutions offer considerable improvement over SR-LS solutions, and, as expected, in most cases hybrid IRWSR-LS solutions provide further but only incremental improvement. This is not surprising because the IRWSR-LS solutions themselves are already fairly close to the solutions of problem (2.2). It should also be noted again that for the exact source location $\boldsymbol{x}_s$ we have $f(\boldsymbol{x}_s) = \sum_{i=1}^{m} \varepsilon_i^2$. One might argue that the SR-LS solution already provides a rather good approximation for R-LS in the sense that SR-LS and IRWSR-LS (hybrid IRWSR-LS) have the same order of magnitude of the mean squared error. However, further analysis of the data that was used to generate Table 2.1 illustrates the advantage of the IRWSR-LS (hybrid IRWSR-LS) solution over the SR-LS.

Each entry in Table 2.2 is a standard deviation of the squared estimation errors aggregated over the same 1,000 Monte Carlo runs described above in Table 2.1 (where the MSE of the position estimation are shown). The results summarised in Table 2.2 demonstrate again that IRWSR-LS and hybrid IRWSR-LS outperform SR-LS. Figures 2.2 - 2.5 describe the histograms of the location estimation errors $\|\boldsymbol{x}^* - \boldsymbol{x}_s\|$ of the SR-LS solution (left images) and IRWSR-LS (right images) for all four noise levels with σ being one of $\{10^{-3}, 10^{-2}, 10^{-1}, 1\}$, where $\boldsymbol{x}^*$ denotes the estimated location and $\boldsymbol{x}_s$ is the exact location of the source. Note that the histograms that correspond to the results obtained by IRWSR-LS are shifted closer towards 0 than those obtained by SR-LS and have smaller variance, and the solutions obtained by running IRWSR-LS have fewer outliers.

Table 2.2: Standard deviation of the squared estimation error for SR-LS, IRWSR-LS and *hybrid* IRWSR-LS methods

σ	SR - LS	IRWSR-LS	*hybrid* IRWSR-LS
1e-03	6.3438e-06	2.0843e-06	2.0864e-06
1e-02	3.2575e-04	2.0530e-04	2.0530e-04
1e-01	4.6998e-02	2.1377e-02	2.1377e-02
1e+0	1.1920e+00	4.3266e+00	4.3266e+00

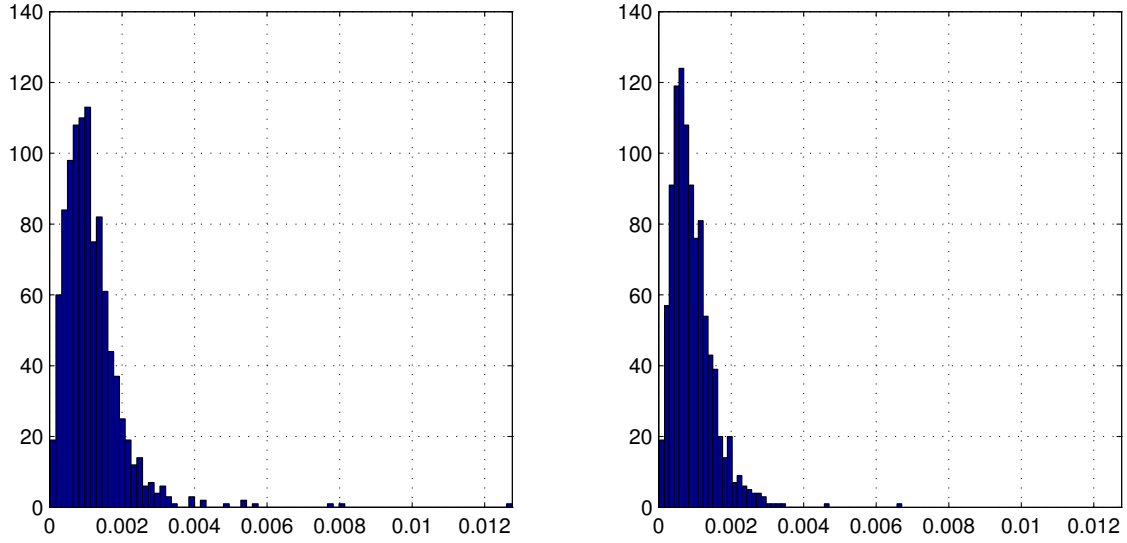

Figure 2.2: Histograms of the errors of the SR-LS (left) and IRWSR-LS (right) solutions, noise $\sigma = 10^{-3}$

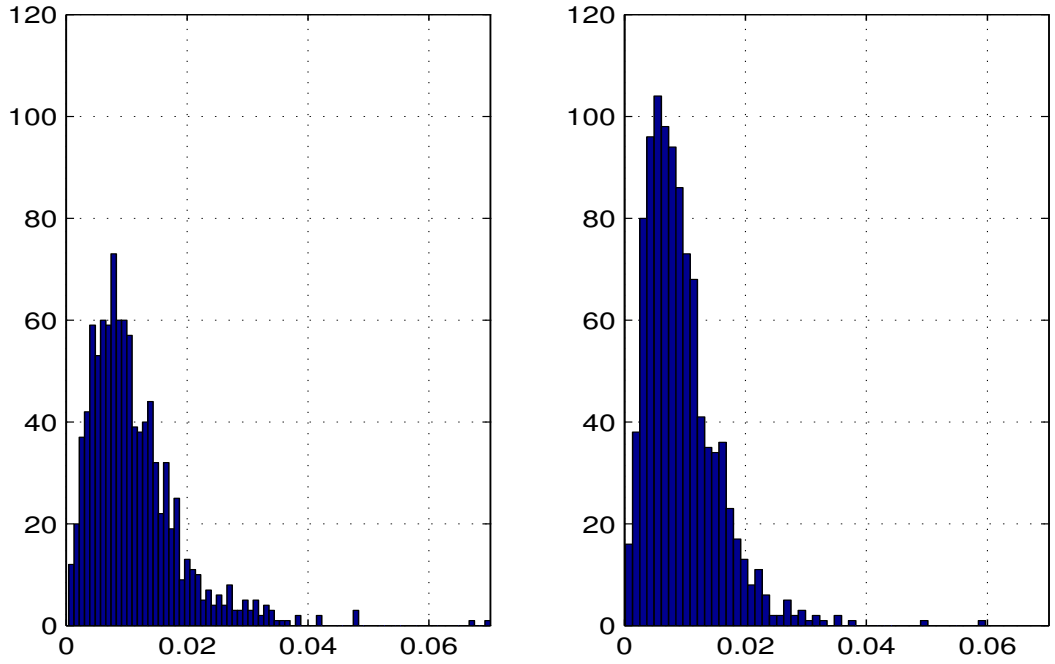

Figure 2.3: Histograms of the errors of the SR-LS (left) and IRWSR-LS (right) solutions, noise $\sigma = 10^{-2}$

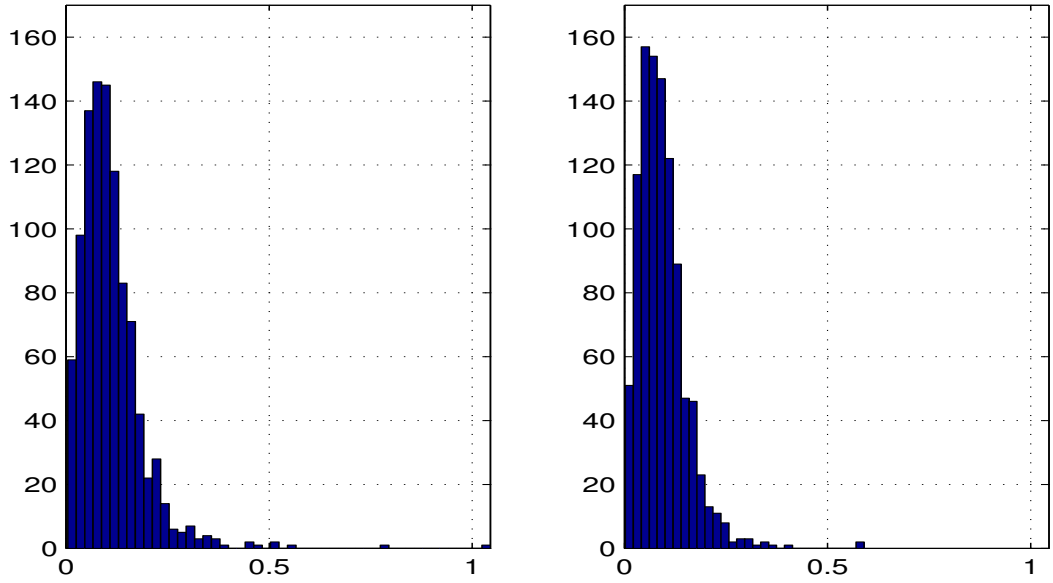

Figure 2.4: Histograms of the errors of the SR-LS (left) and IRWSR-LS (right) solutions, noise $\sigma = 10^{-1}$

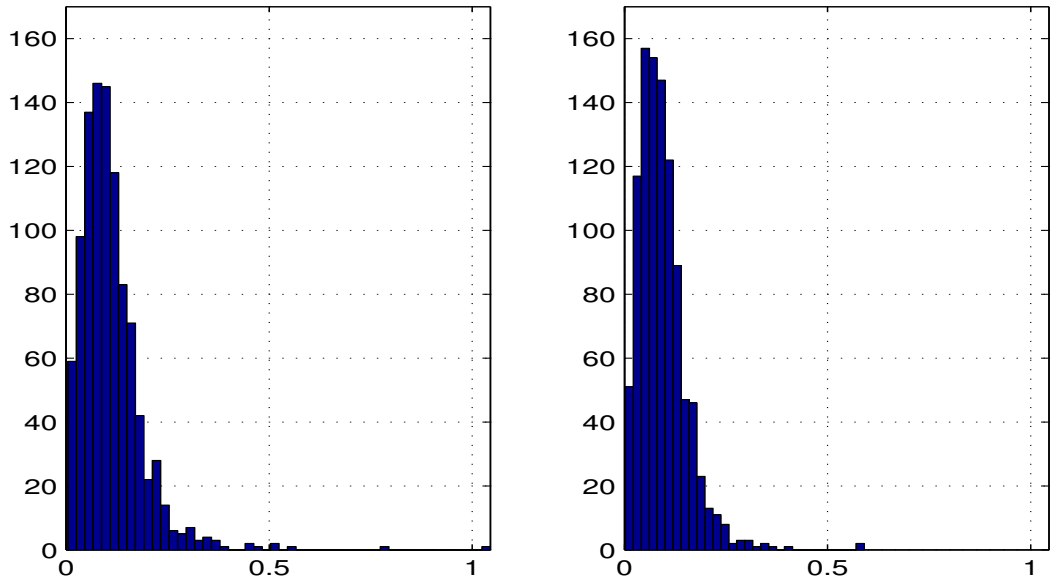

Figure 2.5: Histograms of the errors of the SR-LS (left) and IRWSR-LS (right) solutions, noise $\sigma = 1$

2.2 Source Localization From Range-Difference Measurements

2.2.1 Problem Formulation

Another type of source localization problem that has attracted considerable attention is that of localizing a radiating source using range-difference measurements [14, 15]. In practice, range-difference measurements may be obtained from the time differences of arrival measured by an array of passive sensors. Time difference of arrival (TDOA) is a time-based positioning method based on the idea that the location of an active mobile unit (source of the signal) can be determined by examining the difference in time at which the signal arrives at multiple reference points. Adopting this technique is useful in practical scenarios where synchronization between mobile units is not available [35]. Typical example of such setup includes the observed time difference of arrival (O-TDOA) technique used in 3G (WCDMA) and LTE networks to estimate the location of mobile units. In WCDMA networks only the base stations are synchronized with each other, but the mobile unit is unsynchronized with base stations.

Each TDOA measurement constrains the location of the signal source to be on a hyperboloid with a constant range-difference between the two reference points. A TDOA measurement between base stations BS_i and BS_0 can be given by

$$t_{i0} = (t_i - t_x) - (t_0 - t_x) = t_i - t_0$$

where t_x is the clock time of the mobile unit, t_i and t_0 are the time of arrival between the mobile unit and stations BS_i and BS_0 respectively. The equation can be written in terms of distance (range-difference) through scaling

$$r_i = (t_i - t_0)c = r_i - r_0 = \|\boldsymbol{a}_i - \boldsymbol{x}\| - \|\boldsymbol{a}_0 - \boldsymbol{x}\|, i = 1, \ldots, m$$

where c is the speed of signal propagation, r_i is the distance from station $\boldsymbol{a}_i$ to source $\boldsymbol{x}$, r_0 is the distance from station $\boldsymbol{a}_0$ to source $\boldsymbol{x}$, and $\boldsymbol{a}_i \in R^n$, $n = 2$ or 3, contains coordinates of the ith base station. Without loss of generality, the latter equation is valid with the assumption that the station BS_0 is placed at the origin of the coordinate system, i.e. $\boldsymbol{a}_0 = \boldsymbol{0}$ and used as a *reference* station [35].

The localization problem here is to estimate the location of a radiating source $\boldsymbol{x}$ given the locations of the $m + 1$ sensors $\{\boldsymbol{a}_i, i = 0, 1, \ldots, m\}$ and noise-contaminated

range-difference measurements $\{d_i, i = 1, 2, \ldots, m\}$ where

$$d_i = r_i + \varepsilon_i = \|\boldsymbol{a}_i - \boldsymbol{x}\| - \|\boldsymbol{x}\| + \varepsilon_i, \text{ for } i = 1, 2, \ldots, m \tag{2.21}$$

Therefore, the standard range-difference LS (RD-LS) problem is formulated as

$$\underset{\boldsymbol{x} \in R^n}{\text{minimize}}\, F(\boldsymbol{x}) = \sum_{i=1}^{m} \left(d_i + \|\boldsymbol{x}\| - \|\boldsymbol{x} - \boldsymbol{a}_i\|\right)^2 \tag{2.22}$$

Unfortunately, finding the global solution of (2.22) turns out to be a very hard problem. Nonlinear least squares (NLLS) algorithm [27] is widely used in TDOA localization systems for its performance. If the range measurement errors can be modeled as an additive white Gaussian noise, the accuracy of NLLS approaches the Cramér-Rao lower bound (CRLB). However, NLLS is not guaranteed to converge [13], [27] if the initial position is chosen far away from the actual source location. This becomes a more serious problem when the system coverage area is large since it becomes more difficult to fix one initial position that is close enough to the *unknown* source location. Scaling by MAjorizing a COmplicated Function (SMACOF) strategy [28] can also be applied for position estimation. Compared with NLLS, it is not sensitive to the choice of the initial position and the mean-square error is guaranteed to decrease at each iteration, but it converges significantly slower. Reference [15] proposes a squared range-difference LS (SRD-LS) approach to address this problem, which is summarized below.

By writing (2.21) as $d_i + \|\boldsymbol{x}\| = \|\boldsymbol{x} - \boldsymbol{a}_i\|$ and squaring both sides, we obtain

$$\left(d_i + \|\boldsymbol{x}\|\right)^2 = \|\boldsymbol{x} - \boldsymbol{a}_i\|^2 \tag{2.23}$$

which can be simplified to

$$-2d_i\|\boldsymbol{x}\| - 2\boldsymbol{a}_i^T\boldsymbol{x} = g_i, i = 1, \ldots, m \tag{2.24}$$

where $g_i = d_i^2 - \|\boldsymbol{a}_i\|^2$. In practice (2.24) does not hold exactly due to measurement noise that contaminates the data d_i's. In other words, if d_i's in (2.24) are taken to be real-world data, then we only have

$$-2d_i\|\boldsymbol{x}\| - 2\boldsymbol{a}_i^T\boldsymbol{x} - g_i \approx 0, i = 1, \ldots, m \tag{2.25}$$

Reference [15] proposes a LS solution for the problem at hand by minimizing the sum of squared residues on the left side of (2.25), namely,

$$\underset{\boldsymbol{x}\in R^n}{\text{minimize}} \sum_{i=1}^{m} \left(-2\boldsymbol{a}_i^T\boldsymbol{x} - 2d_i\|\boldsymbol{x}\| - g_i\right)^2 \tag{2.26}$$

By introducing new variable $\boldsymbol{y} = [\boldsymbol{x}^T \|\boldsymbol{x}\|]^T$ and noticing nonnegativity of the component y_{n+1} problem (2.26) is converted to

$$\underset{\boldsymbol{y}\in R^{n+1}}{\text{minimize}} \|\boldsymbol{B}\boldsymbol{y} - \boldsymbol{g}\|^2 \tag{2.27a}$$

$$\text{subject to: } \boldsymbol{y}^T\boldsymbol{C}\boldsymbol{y} = 0 \tag{2.27b}$$

$$y_{n+1} \geq 0 \tag{2.27c}$$

where $\boldsymbol{g} = [g_1 \dots g_m]^T$ and

$$\boldsymbol{B} = \begin{pmatrix} -2\boldsymbol{a}_1^T & -2d_1 \\ \vdots & \vdots \\ -2\boldsymbol{a}_m^T & -2d_m \end{pmatrix}, \boldsymbol{C} = \begin{pmatrix} \boldsymbol{I}_n & \boldsymbol{0}_{n\times 1} \\ \boldsymbol{0}_{1\times n} & -1 \end{pmatrix}$$

Because of the presence of the nonnegativity constraint in (2.27c), (2.27) is no longer a GTRS problem hence the technique used for the case of range measurements does not apply. Nevertheless reference [15] presents a rigorous argument which shows that the optimal solution of (2.27) either assumes the form of

$$\tilde{\boldsymbol{y}}(\lambda) = \left(\boldsymbol{B}^T\boldsymbol{B} + \lambda\boldsymbol{C}\right)^{-1}\boldsymbol{B}^T\boldsymbol{g} \tag{2.28}$$

where λ solves

$$\tilde{\boldsymbol{y}}(\lambda)^T\boldsymbol{C}\tilde{\boldsymbol{y}}(\lambda) = 0 \tag{2.29}$$

and makes $\boldsymbol{B}^T\boldsymbol{B} + \lambda\boldsymbol{C}$ positive definite, or is the vector among $\{\boldsymbol{0}, \tilde{\boldsymbol{y}}(\lambda_1), \dots, \tilde{\boldsymbol{y}}(\lambda_p)\}$ that gives the smallest objective function in (2.27a), where $\{\lambda_i, i = 1, \dots, p\}$ are all roots of (2.29) such that the $(n+1)$'th component of $\tilde{\boldsymbol{y}}(\lambda_i)$ is nonnegative and $\boldsymbol{B}^T\boldsymbol{B} + \lambda\boldsymbol{C}$ has exactly one negative and n positive eigenvalues. We shall refer the global solution of (2.27) to as the SRD-LS solution.

2.2.2 Improved Solution Using Iterative Re-weighting

The Algorithm

We now present a method for improved solutions over SRD-LS solutions. The method incorporates an iterative re-weighting procedure into the SRD-LS approach, hence it is in spirit similar to the IRWRS-LS approach described in Sec. 2.1.2. We begin by considering the weighted SRD-LS problem

$$\underset{\boldsymbol{x}\in R^n}{\text{minimize}} \sum_{i=1}^{m} w_i \left(-2\boldsymbol{a}_i^T\boldsymbol{x} - 2d_i\|\boldsymbol{x}\| - g_i\right)^2 \tag{2.30}$$

where weights w_i for $i = 1, \ldots, m$ are fixed nonnegative constants. The counterpart of (2.28) for the problem (2.30) is given by

$$\underset{\boldsymbol{y}\in R^{n+1}}{\text{minimize}} \|\boldsymbol{B}_w\boldsymbol{y} - \boldsymbol{g}_w\| \tag{2.31a}$$

$$\text{subject to: } \boldsymbol{y}^T\boldsymbol{C}\boldsymbol{y} = 0 \tag{2.31b}$$

$$y_{n+1} \geq 0 \tag{2.31c}$$

where $\boldsymbol{B}_w = \boldsymbol{\Gamma}\boldsymbol{B}$, $\boldsymbol{g}_w = \boldsymbol{\Gamma}\boldsymbol{g}$ and $\boldsymbol{\Gamma} = \text{diag}\{\sqrt{w_1}, \ldots, \sqrt{w_m}\}$, which will be referred to as the weighted SRD-LS (WSRD-LS) problem. On comparing (2.31) with (2.28), it follows immediately that the global solver for problem (2.28) characterized by data set $\{\boldsymbol{B}, \boldsymbol{g}, \boldsymbol{C}\}$ can also be sued for solving problem (2.31) be used applying it to data set $\{\boldsymbol{B}_w, \boldsymbol{g}_w, \boldsymbol{C}\}$.

Concerning the assignment of weights $\{w_i, i = 1, \ldots, w_m\}$, we recall (2.23), (2.24) and observe that the ith term of the objective function in (2.30) can be written as

$$\begin{aligned} & w_i \left(-2d_i\|\boldsymbol{x}\| - 2\boldsymbol{a}_i^T\boldsymbol{x} - g_i\right)^2 \\ =& w_i \left((d_i + \|\boldsymbol{x}\|)^2 - \|\boldsymbol{x} - \boldsymbol{a}_i\|^2\right)^2 \\ =& w_i \left(d_i + \|\boldsymbol{x}\| + \|\boldsymbol{x} - \boldsymbol{a}_i\|\right)\left(d_i + \|\boldsymbol{x}\| - \|\boldsymbol{x} - \boldsymbol{a}_i\|\right) \end{aligned}$$

Clearly, the last expression above would become the ith term of the objective function in the RD-LS problem (2.22) if weights w_i were set to

$$\frac{1}{\left(d_i + \|\boldsymbol{x}\| + \|\boldsymbol{x} - \boldsymbol{a}_i\|\right)^2}$$

so that the first two factors are cancelled out. This suggests that a realizable weight

assignment for performing practically the same cancellation can be made by means of iterative re-weighting for problems (2.30) and (2.31) where the weights in the kth iteration are assigned to

$$w_i^{(k)} = \frac{1}{\left(d_i + \|\boldsymbol{x}_{k-1}\| + \|\boldsymbol{x}_{k-1} - \boldsymbol{a}_i\|\right)^2}, i = 1, \ldots, m \tag{2.32}$$

Based on the analysis above, a localization algorithm for range-difference measurements can be outlined as follows.

Algorithm 2

1) Input data: Sensor locations $\{\boldsymbol{a}_i, i = 0, 1, \ldots, m\}$ with $\boldsymbol{a}_0 = \boldsymbol{0}$, range-difference measurements $\{d_i, i = 1, \ldots, m\}$, maximum number of iterations k_{max} and convergence tolerance ξ.

2) Generate data set $\{\boldsymbol{B}, \boldsymbol{g}, \boldsymbol{C}\}$ as

$$\boldsymbol{g} = \begin{pmatrix} d_1^2 - \|\boldsymbol{a}_1\|^2 \\ \vdots \\ d_m^2 - \|\boldsymbol{a}_m\|^2 \end{pmatrix}, \boldsymbol{B} = \begin{pmatrix} -2\boldsymbol{a}_1^T & -2d_1 \\ \vdots & \vdots \\ -2\boldsymbol{a}_m^T & -2d_m \end{pmatrix}, \boldsymbol{C} = \begin{pmatrix} \boldsymbol{I}_n & \boldsymbol{0}_{n\times 1} \\ \boldsymbol{0}_{1\times n} & -1 \end{pmatrix}.$$

Set $k = 1$, $w_i^{(1)} = 1$ for $i = 1, \ldots, m$.

3) Set $\boldsymbol{\Gamma}_k = \text{diag}\left(\sqrt{w_1^{(k)}}, \ldots, \sqrt{w_m^{(k)}}\right)$, $\boldsymbol{B}_w = \boldsymbol{\Gamma}_k \boldsymbol{B}$ and $\boldsymbol{g}_w = \boldsymbol{\Gamma}_k \boldsymbol{g}$.

4) Solve WSRD-LS problem

$$\begin{aligned} \underset{\boldsymbol{y}\in R^{n+1}}{\text{minimize}} \; & \|\boldsymbol{B}_w \boldsymbol{y} - \boldsymbol{g}_w\| \\ \text{subject to: } & \boldsymbol{y}^T \boldsymbol{C} \boldsymbol{y} = 0 \\ & y_{n+1} \geq 0 \end{aligned}$$

to obtain its global solution $\boldsymbol{x}_k$.

5) If $k = k_{max}$ or $\|\boldsymbol{x}_k - \boldsymbol{x}_{k-1}\| < \xi$, terminate and output $\boldsymbol{x}_k$ as the solution; otherwise, set $k = k + 1$, update weights $\{w_i^{(k)}, i = 1, \ldots, m\}$ as

$$w_i^{(k)} = \frac{1}{\left(d_i + \|\boldsymbol{x}_{k-1}\| + \|\boldsymbol{x}_{k-1} - \boldsymbol{a}_i\|\right)^2}$$

and repeat from Step 3).

It is evident that the complexity of the algorithm is practically equal to the complexity of the WSRD-LS solver involved in Step 4 times the number of iterations, k, which is typically in the range of 3 to 6. We shall call the solutions obtained from Algorithm 2 IRWSRD-LS solutions. Technical details on how to solve (2.31) can be found in Appendix 1.

A variant of Algorithm 2

Like in the case of range measurements, once the IRWSRD-LS solution is obtained by applying Algorithm 2, which is expected to be within a small vicinity of the true global solution of the RD-LS problem (2.22), the gap can be closed by running a good local method that takes the IRWSRD-LS solution as an initial point. Again, the Newton method is chosen for its fast convergence, low complexity due to the extremely low dimension n, and the availability of closed-form formulas to compute the gradient and Hessian of $F(\boldsymbol{x})$ in (2.22).

Assuming $\boldsymbol{x} \neq \boldsymbol{a}_i$ for $i = 0, 1, \ldots, m$, the gradient and Hessian of $F(\boldsymbol{x})$ is found to be

$$\boldsymbol{g}(\boldsymbol{x}) = \sum_{i=1}^{m} c_i \left(\boldsymbol{q}_i - \tilde{(}\boldsymbol{x}) \right)$$

and

$$\boldsymbol{H}(\boldsymbol{x}) = \sum_{i=1}^{m} \left[(\boldsymbol{q}_i - \tilde{(}\boldsymbol{x}))(\boldsymbol{q}_i - \tilde{(}\boldsymbol{x}))^T + c_i(\boldsymbol{Q}_{1i} + \boldsymbol{Q}_2) \right]$$

respectively, where

$$c_i = \|\boldsymbol{x} - \boldsymbol{a}_i\| - \|\boldsymbol{x}\|, \boldsymbol{q}_i = \frac{\boldsymbol{x} - \boldsymbol{a}_i}{\|\boldsymbol{x} - \boldsymbol{a}_i\|}, \tilde{\boldsymbol{x}} = \frac{\boldsymbol{x}}{\|\boldsymbol{x}\|}$$

and

$$\boldsymbol{Q}_{1i} = \frac{1}{\|\boldsymbol{x} - \boldsymbol{a}_i\|} \left(\boldsymbol{I} - \boldsymbol{q}_i \boldsymbol{q}^T \right), \boldsymbol{Q}_2 = \frac{1}{\|\boldsymbol{x}\|} \left(\boldsymbol{I} - \tilde{\boldsymbol{x}} \tilde{\boldsymbol{x}}^T \right)$$

To ensure the positive definiteness of Hessian, eigen decomposition of $\boldsymbol{H}(\boldsymbol{x})$, namely,

$$\boldsymbol{H}(\boldsymbol{x}) = \boldsymbol{U} \boldsymbol{\Lambda} \boldsymbol{U}^T$$

may be performed, where $\boldsymbol{U}$ is orthogonal and $\boldsymbol{\Lambda} = \text{diag}(\lambda_1, \ldots, \lambda_n)$ with $\{\lambda_i, i = 1, \ldots, n\}$ being the eigenvalues of $\boldsymbol{H}(\boldsymbol{x})$. Let λ_{min} be the smallest eigenvalue of $\boldsymbol{H}(\boldsymbol{x})$. If λ_{min}, then $\boldsymbol{H}(\boldsymbol{x})$ is positive definite and the Newton algorithm is carried

out without modification; if $\lambda_{min} \leq 0$, then the algorithm uses a slightly modified Hessian given by

$$\tilde{\boldsymbol{H}}(\boldsymbol{x}) = \boldsymbol{U}\tilde{\boldsymbol{\Lambda}}\boldsymbol{U}^T$$

where $\tilde{\boldsymbol{\Lambda}} = \text{diag}\left(\tilde{\lambda}_1, \ldots, \tilde{\lambda}_n\right)$ with

$$\tilde{\lambda}_i = \begin{cases} \lambda_i & \text{if } \lambda_i > 0 \\ \delta & \text{if } \lambda_i \leq 0 \quad i = 1, \ldots, m \end{cases}$$

and δ a small positive constant. Obviously, $\tilde{\boldsymbol{H}}(\boldsymbol{x})$ is guaranteed to be positive definite. In what follows, solutions obtained by the proposed two-step method are called *hybrid* IRWSRD-LS solutions.

2.2.3 Numerical Results

Performance of the proposed algorithms was evaluated and compared with the method of [15] by Monte Carlo simulations with a set-up similar to that of [15]. SRD-LS solutions were used as performance benchmarks for Algorithm 2 and its variant. In both cases the system consisted of m sensors $\{\boldsymbol{a}_i, i = 1, 2, \ldots, m\}$ randomly placed in the planar region in R^2, and a radiating source $\boldsymbol{x}_s$, located randomly in the region $\{\boldsymbol{x} = [x_1; x_2], -10 \leq x_1, x_2 \leq 10\}$. The coordinates of the source and sensors were generated for each dimension following a uniform distribution. Measurement noise $\{\varepsilon_i, i = 1, \ldots, m\}$ was modelled as independent and identically distributed (i.i.d) random variables with zero mean and variance σ^2. Accuracy of source location estimation was evaluated in terms of mean squared error in the form MSE $= E\{\|\boldsymbol{x}^* - \boldsymbol{x}_s\|\}$ where $\boldsymbol{x}_s$ denotes the exact source location and $\boldsymbol{x}^*$ is its estimation obtained by SRD-LS, IRWSRD-LS and *hybrid* IRWSRD-LS methods, respectively. Table 2.3 provides comparisons of these methods with SRD-LS, where each entry was averaged MSE over 1,000 Monte Carlo runs of the method. For the columns representing performance of the IRWSDR-LS and *hybrid* IRWSDR-LS methods each table entry lists their MSE and relative improvement over SRD-LS solutions in percentage, in the format: MSE(% Improvement).

The simulation studies of Algorithm 2 considered $m = 11$ sensors $\{\boldsymbol{a}_i, i = 1, 2, \ldots, 10\}$ with $\boldsymbol{a}_0 = \boldsymbol{0}$ and other ten sensors placed in the region $[-15; 15] \times [-15; 15]$, with σ being one of five possible levels $\{10^{-4}, 10^{-3}, 10^{-2}, 10^{-1}, 1\}$. The range-difference measurements used to form matrix $\boldsymbol{B}$ in Step 2 of the Algorithm 2 were calculated as

Table 2.3: MSE of position estimation for SRD-LS, IRWSRD-LS and *hybrid* IRWSRD-LS methods

σ	SR - LS	IRWSR-LS (Im.,%)	*hybrid* IRWSR-LS (Im.,%)
1e-04	1.3830e-08	8.2271e-09 (40)	8.2270e-09 (40)
1e-03	1.3063e-06	8.2828e-07 (37)	8.2827e-07 (37)
1e-02	1.1163e-04	6.6779e-05 (40)	6.6779e-05 (40)
1e-01	1.2095e-02	7.2089e-03 (40)	7.2089e-03 (40)
1e+0	1.5705e+00	9.7075e-01 (38)	9.7075e-01 (38)

Table 2.4: Standard deviation of the squared estimation error for SRD-LS, IRWSRD-LS and *hybrid* IRWSRD-LS methods

σ	SR - LS	IRWSR-LS	*hybrid* IRWSR-LS
1e-04	4.5624e-08	2.2446e-08	2.2446e-08
1e-03	3.9506e-06	3.1610e-06	3.1610e-06
1e-02	2.2710e-04	1.2812e-04	1.2812e-04
1e-01	3.0108e-02	1.8891e-02	1.8891e-02
1e+0	4.5781e+00	3.0597e+00	3.0597e+00

a noise-contaminated range-difference measurements d_i in (2.21).Step 4 of Algorithm 2 was carried out using the SRD-LS algorithm in [15]. Again, the IRWSRD-LS solutions offer considerable improvement over SRD-LS solutions. Further analysis of the data that was used to generate Table 2.3 illustrates the advantage of the IRWSR-LS (hybrid IRWSR-LS) solution over the SR-LS.

Each entry in Table 2.4 is a standard deviation of the squared estimation errors aggregated over the same 1,000 Monte Carlo runs described above in Table 2.3 (where the MSE of the position estimation are shown). The results summarised in Table 2.4 suggest that, again, IRWSR-LS and hybrid IRWSR-LS outperform SR-LS. Figures (2.6 - 2.10) describe the histograms of the location estimation errors $\|\boldsymbol{x}^* - \boldsymbol{x}_s\|$ of the SR-LS solution (left images) and IRWSR-LS (right images) for all four noise levels with σ being one of $\{10^{-3}, 10^{-2}, 10^{-1}, 1\}$. Here $\boldsymbol{x}^*$ denotes the estimated location and $\boldsymbol{x}_s$ is the exact location of the source. Histograms that correspond to the results

obtained by IRWSR-LS are shifted closer towards 0 than those obtained by SR-LS, have smaller variance, and in most cases have fewer outliers with large error.

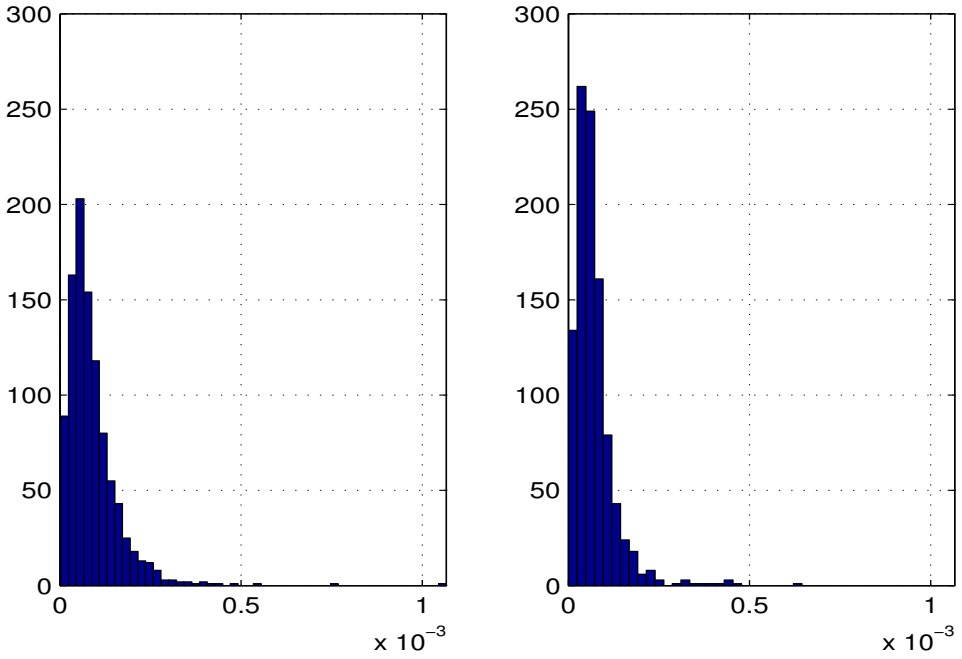

Figure 2.6: Histograms of the errors of the SR-LS (left) and IRWSR-LS (right) solutions, noise $\sigma = 10^{-4}$

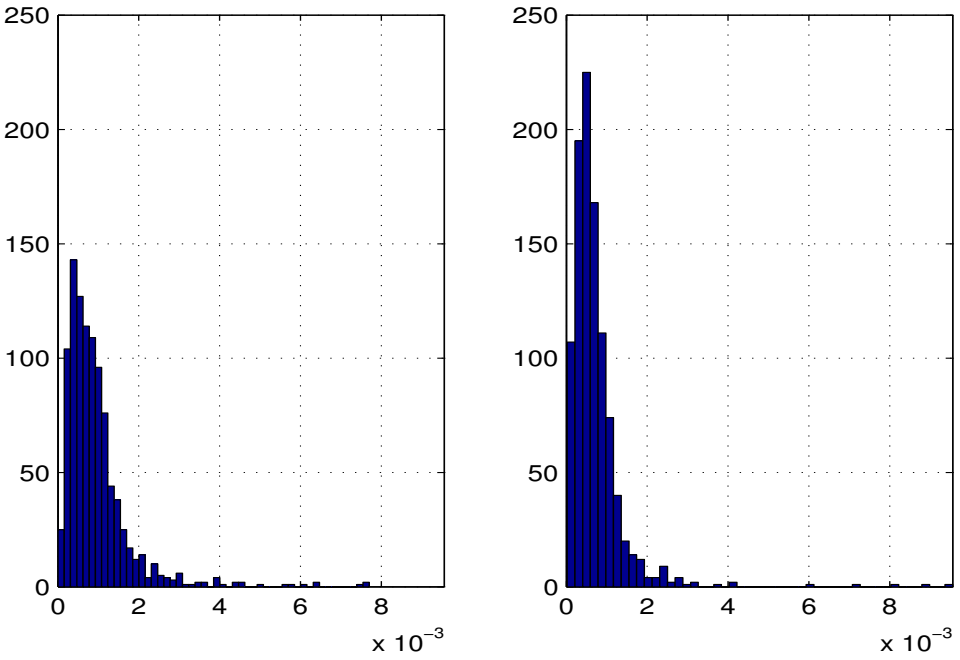

Figure 2.7: Histograms of the errors of the SR-LS (left) and IRWSR-LS (right) solutions, noise $\sigma = 10^{-3}$

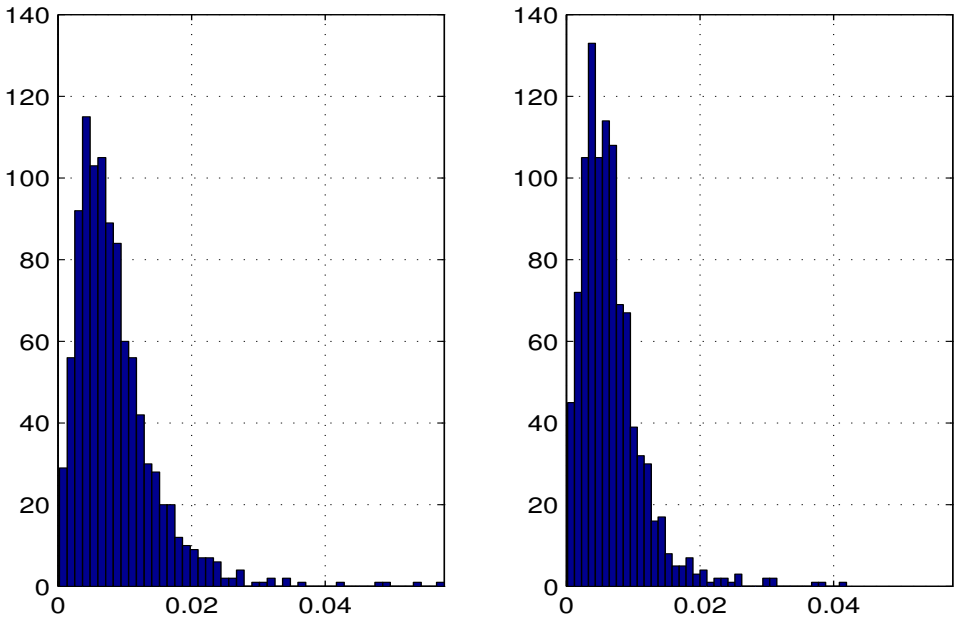

Figure 2.8: Histograms of the errors of the SR-LS (left) and IRWSR-LS (right) solutions, noise $\sigma = 10^{-2}$

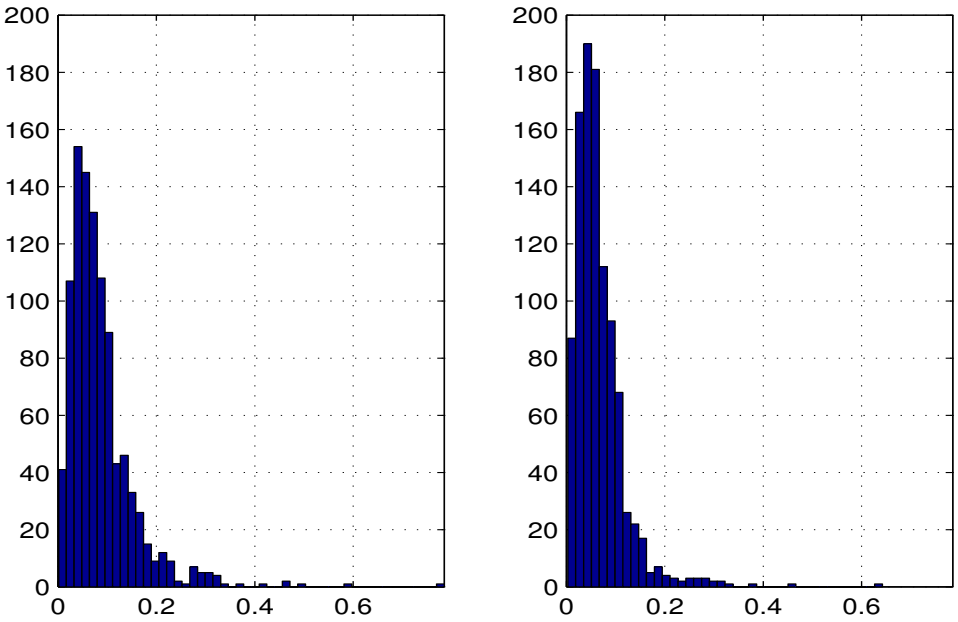

Figure 2.9: Histograms of the errors of the SR-LS (left) and IRWSR-LS (right) solutions, noise $\sigma = 10^{-1}$

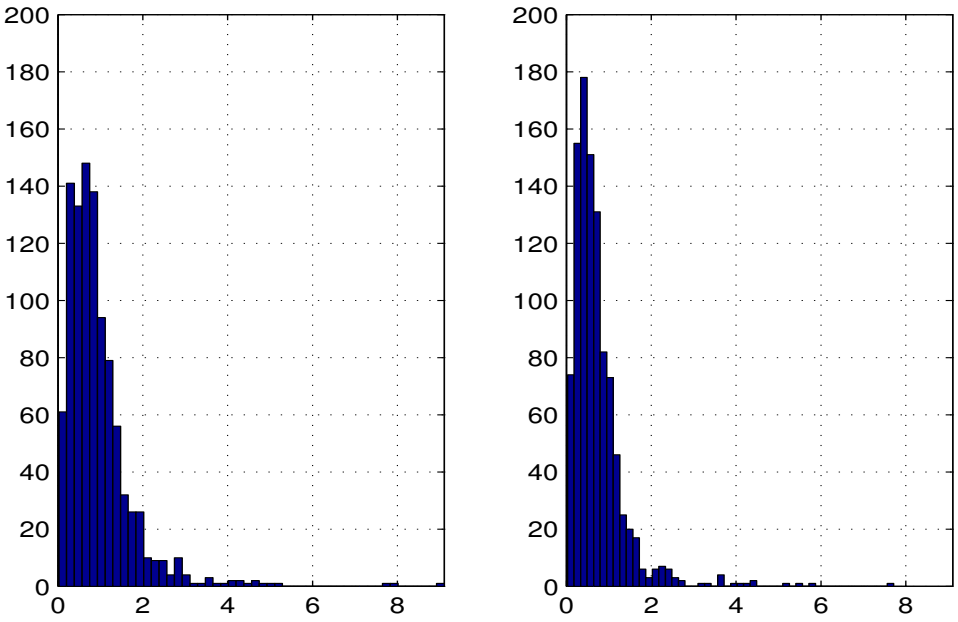

Figure 2.10: Histograms of the errors of the SR-LS (left) and IRWSR-LS (right) solutions, noise $\sigma = 1$

2.3 Extensions

Methods developed in this chapter for localization based on range measurements can be adopted to solve the problem of signle sourse localization from energy measurements [14]. Energy-based source localization, advocated in [7], [9], is motivated by a simple observation that the sound level decreases when the distance between sound source and the listener becomes large. By modeling the relation between sound level (energy) and distance from the sound source, one may estimate the source location using multiple energy readings at different known sensor locations. When the sound is propagating through the air, it is known that the acoustic energy emitted omnidirectionally from a sound source will attenuate at a rate that is inversely proportional to the square of the distance [7]. Using this fact and some simple manipulations, it is possible to obtain an equation in the vector of unknow source location $\boldsymbol{x}$ that is somewhat similar to (2.9). The rest of the section provides technical details of this reformulation.

2.3.1 Acoustic Energy Attenuation Model

Let m be a number of acoustic sensors. For consistency of notation, let $\boldsymbol{a}_i$ denote the known location of the sensor i in space R^n, $n = 2$ or 3. Each sensor measures the acoustic intensity radiated by a source $\boldsymbol{x} \in R^n$ over a time period $T = \frac{M}{f_s}$, where M is the number of sample points used for estimating the acoustic enery and f_s is the sampling frequency. Acoustic energy received by sensor i over a time period T can be represented as:

$$r_i = g_i \frac{S}{\|\boldsymbol{x} - \boldsymbol{a}_i\|^\alpha} + \varepsilon_i \tag{2.33}$$

where $\|\boldsymbol{x} - \boldsymbol{a}_i\|$ is the Euclidean distance between the ith sensor and the source. g_i is a factor that takes into account ith sensor gain. It is asssumed that the gain of individual sensors is either known, i.e. obtained at the sensor callibration stage, or is same for all sensors. S is the unknown acoustic energy measured 1 unit distance away from the source. α is the energy decay factor and is usually assumed to have a value 2 [7]. ε_i denotes the square of the background noise affecting the measurement of sensor i. Based on the central limit theorem, it can be approximated well as a normal distribution, namely, $\varepsilon_i \sim N(\mu_i, \sigma_i^2)$ with a positive mean value μ_i that is no less that the standard deviation σ_i that can be estimated empirically from data samples [7]. More details on derivation and assumptions of this model can be found

in [7][9], [26] and its references.

References [7, 8] argue that the maximum likelihood estimation of the vector of unknown parameters $\boldsymbol{\theta} = [\boldsymbol{x}^T S]^T$ can be obtained my minimizing the quadratic form

$$\underset{\theta}{\text{minimize}} \quad \ell(\boldsymbol{\theta}) = \|\boldsymbol{Z} - S\boldsymbol{H}\| \tag{2.34}$$

where

$$\boldsymbol{H} = \begin{bmatrix} \frac{g_1}{\sigma_1 \|\boldsymbol{x}-\boldsymbol{a}_1\|^2} \\ \frac{g_2}{\sigma_2 |\boldsymbol{x}-\boldsymbol{a}_2\|^2} \\ \vdots \\ \frac{g_m}{\sigma_m |\boldsymbol{x}-\boldsymbol{a}_m\|^2} \end{bmatrix}, \boldsymbol{Z} = \begin{bmatrix} \frac{y_1-\mu_1}{\sigma_1} \\ \frac{y_2-\mu_2}{\sigma_2} \\ \vdots \\ \frac{y_m-\mu_m}{\sigma_m} \end{bmatrix},$$

and $\boldsymbol{Z}$ are (estimated) normalized energy measurements for the case of the single radiating source. Important assumption about (2.34) is that μ_i and σ_i are considered known.

2.3.2 Reformulation

There are two things to note about (2.34). First, (2.34) is a *nonlinear* least square objective function because the vector $\boldsymbol{H}$ is a nonlinear function of the n unknown source coordinates, where n is the dimention of the location coordinates. Second, although there are m sensors reporting the acousting energy reading in fact there are $n + 1 \leq m$ unknowns, including the unknown acoustic energy S radiated from the source. To eliminate the unknown source energy S [8] propose first to compute the ratio k_{ij} of the calibrated energy readings from ith and jth sensor as

$$k_{ij} = \left[\frac{z_i/g_i}{z_j/g_j}\right]^{-1/\alpha} = \frac{\|\boldsymbol{x} - \boldsymbol{a}_i\|}{\|\boldsymbol{x} - \boldsymbol{a}_j\|} \tag{2.35}$$

for $i = 1, 2, \ldots, m-1$, and $j = i+1, \ldots, m$. For the case $0 < k_{ij} \neq 1$ all possible source coordinates $\boldsymbol{x}$ that form a solution to (2.35) reside on a n-dimensional hyper-sphere described by the equation:

$$\|\boldsymbol{x} - \boldsymbol{c}\|^2 = \rho_{ij}^2 \tag{2.36}$$

where the center $\boldsymbol{c}_{ij}$ and the radius ρ_{ij} of the hyper-sphere associated with the sensors i and j are given by:

$$\boldsymbol{c}_{ij} = \frac{\boldsymbol{a}_i - k_{ij}^2 \cdot \boldsymbol{a}_j}{1 - k_{ij}^2}, \rho_{ij} = \frac{k_{ij}\|\boldsymbol{a}_i - \boldsymbol{a}_j\|}{1 - k_{ij}^2} \tag{2.37}$$

For the case when $k_{ij} \to 1$ the possible source locations $\boldsymbol{x}$ reside on the hyperplane between sensors $\boldsymbol{a}_i$ and $\boldsymbol{a}_j$:

$$\boldsymbol{x}^T \boldsymbol{\gamma}_{ij} = \tau_{ij}$$

where $\boldsymbol{\gamma}_{ij} = \boldsymbol{a}_i - \boldsymbol{a}_j$ and $\tau_{ij} = (\|\boldsymbol{a}_i\|^2 - \|\boldsymbol{a}_j\|^2)/2$.

Let I_1 and I_2 be two index sets such that $0 < k_{ij} \neq 1$ for all $\{i, j\} \in I_1$ and $k_{ij} = 1$ for all $\{i, j\} \in I_2$ with $1 \leq i \leq m-1, i+1 \leq j \leq m$ and $I_1 \cap I_2 = \emptyset$. Let L_1 and L_2 denote the number of elements in sets I_1 and I_2 respectively (number of hyperspheres and hyperplanes) and $L_1 + L_2 = m(m-1)/2$. Then the unknown location of the source can be found via minimization of the criterion that is equivalent to (2.34) [8]:

$$\underset{\boldsymbol{x}}{\text{minimize}} \sum_{l_1=1}^{L_1} \left(\|\boldsymbol{x} - \boldsymbol{c}_{l_1}\|^2 - \rho_{l_1}^2 \right)^2 + \sum_{l_2=1}^{L_2} \left(\boldsymbol{x}^T \boldsymbol{\gamma}_{l_2} - \tau_{l_2} \right)^2 \tag{2.38}$$

For the brevity of notation the double indexes ij were replaced by single indexes l_1 and l_2. After some simple manupilations and necessary variable changes, (2.38) can be converted to the constrained problem that is similar to (2.10):

$$\underset{\boldsymbol{y} \in R^{n+1}}{\text{minimize}} \|\boldsymbol{A}\boldsymbol{y} - \boldsymbol{b}\|^2 \tag{2.39a}$$

$$\text{subject to:} \quad \boldsymbol{y}^T \boldsymbol{D} \boldsymbol{y} + 2\boldsymbol{f}^T \boldsymbol{y} = 0 \tag{2.39b}$$

where

$$\boldsymbol{y} = \begin{bmatrix} \boldsymbol{x} \\ \|\boldsymbol{x}\|^2 \end{bmatrix}, \boldsymbol{A} = \begin{pmatrix} \boldsymbol{A}_1 \\ \boldsymbol{A}_2 \end{pmatrix}, \boldsymbol{b} = \begin{pmatrix} \boldsymbol{b}_1 \\ \boldsymbol{b}_2 \end{pmatrix} \tag{2.40}$$

$$\boldsymbol{D} = \begin{pmatrix} \boldsymbol{I}_{n \times n} & \boldsymbol{0}_{n \times 1} \\ \boldsymbol{0}_{1 \times n} & 0 \end{pmatrix}, \boldsymbol{f} = \begin{pmatrix} \boldsymbol{0} \\ -0.5 \end{pmatrix}$$

and submatrices of $\boldsymbol{A}$ and elements of $\boldsymbol{b}$ are formed as follows:

$$\boldsymbol{A}_1 = \begin{pmatrix} -2\boldsymbol{c}_1^T & 1 \\ \vdots & \vdots \\ -2\boldsymbol{a}_{L_1}^T & 1 \end{pmatrix}, \boldsymbol{b}_1 = \begin{pmatrix} \rho_1^2 - \|\boldsymbol{c}_1\|^2 \\ \vdots \\ \rho_{L_1}^2 - \|\boldsymbol{c}_{L_1}\|^2 \end{pmatrix} \tag{2.41}$$

$$\boldsymbol{A}_2 = \begin{pmatrix} \gamma_1^T & 0 \\ \vdots & \vdots \\ \gamma_{L_2}^T & 0 \end{pmatrix}, \boldsymbol{b}_2 = \begin{pmatrix} \tau_1 \\ \vdots \\ \tau_{L_2} \end{pmatrix}$$

The unconstrained problem in (2.38), due to mathematical analogy with (2.9), can be solved using Algorithm 1 developed in section 3.1.

Chapter 3

Penalty Convex-Concave Procedure for Source Localization Problem

This chapter is focused on the least squares formulation for the problem of localizing a single radiating source based on range measurements. We exploit special structure of the cost function of an unconstrained LS formulation and show that it is well suited for being investigated in a setting known as difference-of-convex-functions (DC) programming. Further, we present an algorithm for solving the LS problem at hand based on a penalty convex-concave procedure (PCCP) [30] that accommodates infeasible initial points. We also provide algorithmic details that are tailored to the localization problem at hand, these include additional constraints that enforce the algorithms iteration path towards the LS solution and strategies to secure good initial points for the algorithm. Numerical results are presented to demonstrate that the proposed algorithm offers substantial performance improvement relative to some best known results from the literature.

3.1 Problem Statement and Review of Related Work

same: *The source localization problem considered here involves a given array of m sensors specified by $\{\boldsymbol{a}_1, \ldots, \boldsymbol{a}_m\}$ where $\boldsymbol{a}_i \in R^n$ contains n coordinates of the ith sensor in space R^n. Each sensor measures its distance to a radiating source $\boldsymbol{x} \in R^n$. Throughout it is assumed that only noisy copies of the distance data are available,*

hence the range measurements obey the model

$$r_i = \|\boldsymbol{x} - \boldsymbol{a}_i\| + \varepsilon_i, \quad i = 1, \ldots, m. \tag{3.1}$$

where ε_i denotes the unknown noise that has occurred when the ith sensor measures its distance to source $\boldsymbol{x}$. Let $\boldsymbol{r} = [r_1\ r_2 \ldots r_m]^T$ and $\boldsymbol{\varepsilon} = [\varepsilon_1\ \varepsilon_2 \ldots \varepsilon_m]^T$, the source localization problem can be stated as to estimate the exact source location $\boldsymbol{x}$ from the noisy range measurements $\boldsymbol{r}$. **In the rest of this section: shorten the review of the problem. add more lit review on methods** For the localization problem at hand, the range-based least squares (R-LS) estimate refers to the solution of the problem

$$\underset{\boldsymbol{x}}{\text{minimize}} \quad F(\boldsymbol{x}) = \sum_{i=1}^{m} (r_i - \|\boldsymbol{x} - \boldsymbol{a}_i\|)^2 \tag{3.2}$$

Formulation (3.2) is connected to the maximum-likelihood (ML) location estimation that determines $\boldsymbol{x}$ by examining the probabilistic model of the error vector $\boldsymbol{\varepsilon}$. If $\boldsymbol{\varepsilon}$ obeys a Gaussian distribution with zero mean and covariance $\boldsymbol{\Sigma} = \text{diag}(\sigma_1^2, \ldots, \sigma_m^2)$, then the maximum likelihood (ML) location estimator in this case is known to be

$$\boldsymbol{x}_{ML} = \arg\min_{\boldsymbol{x} \in R^n} (\boldsymbol{r} - \boldsymbol{g})^T \Sigma^{-1} (\boldsymbol{r} - \boldsymbol{g}) \tag{3.3}$$

where $\boldsymbol{g} = [g_1\ g_2 \ldots\ g_m]^T$ with $g_i = \|\boldsymbol{x} - \boldsymbol{a}_i\|$. It follows immediately that the ML solution in (3.3) is identical to the R-LS solution of problem (3.2) when covariance $\boldsymbol{\Sigma}$ is proportional to the identity matrix, i.e., $\sigma_1^2 = \ldots = \sigma_m^2 = 1$. In the literature this is known as the equal noise power case. For notation simplicity this paper focuses on the equal noise power case, however the method developed below is also applicable to the unequal noise power case by working on a weighted version of the objective in (3.2) with $\{\sigma_i^{-2}, i = 1, \ldots, m\}$ as the weights.

There are many methods for continuous unconstrained optimization [33], however most of them are *local* methods in the sense they are sensitive to the choice of initial point, and give no guarantee to yield global solutions when applied to non-convex objective functions. Unfortunately, the objective function in (3.2) is highly non-convex, possessing many local minimizers even for small-scale systems. In this paper we present an different approach to solve the positioning problem, which employs a successive convex-concave procedure.

Advantages of convex-concave procedure from citeLBoyd

3.2 Fitting the Localization Problem to the CCP Framework

3.2.1 Basic Convex-Concave Procedure

describe what a DC problem is The CCP refers to an effective heuristic method to deal with a class of *nonconvex* problems of the form

$$\begin{aligned} \underset{\boldsymbol{x}}{\text{minimize}} \quad & f(\boldsymbol{x}) - g(\boldsymbol{x}) && \text{(3.4a)} \\ \text{subject to:} \quad & f_i(\boldsymbol{x}) \leq g_i(\boldsymbol{x}) \quad \text{for: } i = 1, 2, \ldots, m && \text{(3.4b)} \end{aligned}$$

where $f(\boldsymbol{x}), g(\boldsymbol{x}), f_i(\boldsymbol{x}), g_i(\boldsymbol{x})$ for $i = 1, 2, \ldots, m$ are convex. The basic CCP algorithm is an iterative procedure including two key steps (in the k-th iteration where iterate $\boldsymbol{x}_k$ is known):

(i) Convexification of the objective function and constraints by replacing $g(\boldsymbol{x})$ and $g_i(\boldsymbol{x})$, respectively, with their affine approximations

$$\hat{g}(\boldsymbol{x}, \boldsymbol{x}_k) = g(\boldsymbol{x}_k) + \bigtriangledown g(\boldsymbol{x}_k)^T (\boldsymbol{x} - \boldsymbol{x}_k) \tag{3.5a}$$

and

$$\hat{g}_i(\boldsymbol{x}, \boldsymbol{x}_k) = g_i(\boldsymbol{x}_k) + \bigtriangledown g_i(\boldsymbol{x}_k)^T (\boldsymbol{x} - \boldsymbol{x}_k) \quad \text{for: } i = 1, 2, \ldots, m \tag{3.5b}$$

(ii) Solving the convex problem

$$\begin{aligned} \underset{\boldsymbol{x}}{\text{minimize}} \quad & f(\boldsymbol{x}) - \hat{g}(\boldsymbol{x}, \boldsymbol{x}_k) && \text{(3.6a)} \\ \text{subject to:} \quad & f_i(\boldsymbol{x}) - \hat{g}_i(\boldsymbol{x}, \boldsymbol{x}_k) \leq 0 && \text{(3.6b)} \\ & \text{for: } i = 1, 2, \ldots, m \end{aligned}$$

Because of the convexity of all the functions involved, it can be shown that the basic CCP is a descent algorithm and the iterates $\boldsymbol{x}_k$ converge to the critical point of the original problem (4) [30]. The basic CCP requires a *feasible* initial point $\boldsymbol{x}_0$ (in the sense that $\boldsymbol{x}_0$ satisfies (6b) for $i = 1, 2, \ldots, m$) to start the procedure. By introducing additional slack variables, a penalty CCP has been adopted to accept infeasible initial points.

3.2.2 Problem Reformulation

We begin by re-writing the objective function in (2) up to a constant as:

$$\begin{aligned} F(\boldsymbol{x}) = m\boldsymbol{x}^T\boldsymbol{x} - 2\boldsymbol{x}^T\sum_{i=1}^{m}\boldsymbol{a}_i \\ - 2\sum_{i=1}^{m} r_i\|\boldsymbol{x}-\boldsymbol{a}_i\| \end{aligned} \tag{3.7}$$

The objective in (7) is not convex. This is because, for points $\boldsymbol{x}$ that are not coincided with $\boldsymbol{a}_i$ for $1 \leq i \leq m$, the Hessian of $F(\boldsymbol{x})$ is given by

$$\begin{aligned} \bigtriangledown^2 F(\boldsymbol{x}) = 2m\boldsymbol{I} + 2\sum_{i=1}^{m}\frac{r_i}{\|\boldsymbol{x}-\boldsymbol{a}_i\|^3}\cdot \\ \cdot\Big((\boldsymbol{x}-\boldsymbol{a}_i)(\boldsymbol{x}-\boldsymbol{a}_i)^T - \|\boldsymbol{x}-\boldsymbol{a}_i\|^2\boldsymbol{I}\Big) \end{aligned}$$

which is not always positive semidefinite. On the other hand, by defining

$$\begin{aligned} f(\boldsymbol{x}) &= m\boldsymbol{x}^T\boldsymbol{x} - 2\boldsymbol{x}^T\sum_{i=1}^{m}\boldsymbol{a}_i \\ g(\boldsymbol{x}) &= 2\sum_{i=1}^{m} r_i\|\boldsymbol{x}-\boldsymbol{a}_i\| \end{aligned} \tag{3.8}$$

the objective in (7) can be expressed as $F(\boldsymbol{x}) = f(\boldsymbol{x}) - g(\boldsymbol{x})$ with both $f(\boldsymbol{x})$ and $g(\boldsymbol{x})$ convex, hence it fits naturally into (4a). Note that $g(\boldsymbol{x})$ in (8) is not differentiable at the point where $\boldsymbol{x} = \boldsymbol{a}_i$ for some $1 \leq i \leq m$, thus we replace the term $\bigtriangledown g(\boldsymbol{x}_k)$ in (5a) by a subgradient [34] of $g(\boldsymbol{x})$ at $\boldsymbol{x}_k$, denoted by $\partial g(\boldsymbol{x}_k)$ as

$$\partial g(\boldsymbol{x}_k) = 2\sum_{i=1}^{m} r_i\partial\|\boldsymbol{x}_k-\boldsymbol{a}_i\|$$

where

$$\partial\|\boldsymbol{x}_k-\boldsymbol{a}_i\| = \begin{cases} \dfrac{\boldsymbol{x}_k-\boldsymbol{a}_i}{\|\boldsymbol{x}_k-\boldsymbol{a}_i\|}, & \text{if } \boldsymbol{x}_k \neq \boldsymbol{a}_i \\ \boldsymbol{0}, & \text{otherwise} \end{cases}$$

Hence $\hat{g}(\boldsymbol{x}, \boldsymbol{x}_k)$ in (5a) is given by

$$\begin{aligned}\hat{g}(\boldsymbol{x}, \boldsymbol{x}_k) &= 2\sum_{i=1}^{m} r_i \|\boldsymbol{x}_k - \boldsymbol{a}_i\| + 2\left(\boldsymbol{x} - \boldsymbol{x}_k\right)^T \sum_{i=1}^{m} r_i \partial\|\boldsymbol{x}_k - \boldsymbol{a}_i\| \\ &= 2\boldsymbol{x}^T \sum_{i=1}^{m} r_i \partial\|\boldsymbol{x}_k - \boldsymbol{a}_i\| + c\end{aligned}$$

where c is a constant given by

$$c = -2\sum_{i=1}^{m} r_i \boldsymbol{a}_i^T \partial\|\boldsymbol{x}_k - \boldsymbol{a}_i\|.$$

It follows that up to a multiplicative factor $1/m$ and an additive constant term the convex objective function in (6a) can be written as

$$\underset{\boldsymbol{x}}{\text{minimize}} \quad \hat{F}(\boldsymbol{x}) = \boldsymbol{x}^T\boldsymbol{x} - 2\boldsymbol{x}^T\boldsymbol{v}_k \tag{3.9}$$

where

$$\boldsymbol{v}_k = \bar{\boldsymbol{a}} + \frac{1}{m}\sum_{i=1}^{m} r_i \partial\|\boldsymbol{x}_k - \boldsymbol{a}_i\|, \quad \bar{\boldsymbol{a}} = \frac{1}{m}\sum_{i=1}^{m} \boldsymbol{a}_i \tag{3.10}$$

It is rather straightforward to see that given $\boldsymbol{x}_k$ (in the k-th iteration) the solution of the quadratic problem (9) can be obtained as

$$\boldsymbol{x}_{k+1} = \bar{\boldsymbol{a}} + \frac{1}{m}\sum_{i=1}^{m} r_i \partial\|\boldsymbol{x}_k - \boldsymbol{a}_i\| \tag{3.11}$$

3.2.3 Imposing Error Bounds and Penalty Terms

The algorithm being developed can be enhanced by imposing a bound on each squared measurement error, namely

$$\left(\|\boldsymbol{x} - \boldsymbol{a}_i\| - r_i\right)^2 \leq \delta_i^2 \tag{3.12}$$

which leads to

$$\|\boldsymbol{x} - \boldsymbol{a}_i\| - r_i - \delta_i \leq 0 \tag{3.13a}$$

$$r_i - \delta_i \leq \|\boldsymbol{x} - \boldsymbol{a}_i\| \tag{3.13b}$$

for $1 \leq i \leq m$. The constraints in (13a) are convex and fit into those in (6b) with $f_i(\boldsymbol{x}) = \|\boldsymbol{x} - \boldsymbol{a}_i\| - r_i - \delta_i$ and $g_i(\boldsymbol{x}) = 0$, while those in (13b) are in the form of (4b) with $f_i(\boldsymbol{x}) = r_i - \delta_i$ and $g_i(\boldsymbol{x}) = \|\boldsymbol{x} - \boldsymbol{a}_i\|$. Following CCP (see (5b)), $g_i(\boldsymbol{x}) = \|\boldsymbol{x} - \boldsymbol{a}_i\|$ is linearized around iterate $\boldsymbol{x}_k$ to

$$\hat{g}_i(\boldsymbol{x}, \boldsymbol{x}_k) = \|\boldsymbol{x}_k - \boldsymbol{a}_i\| + \partial\|\boldsymbol{x}_k - \boldsymbol{a}_i\|^T (\boldsymbol{x} - \boldsymbol{x}_k)$$

and (13b) is convexified as

$$r_i - \delta_i \leq \|\boldsymbol{x}_k - \boldsymbol{a}_i\| + \partial\|\boldsymbol{x}_k - \boldsymbol{a}_i\|^T (\boldsymbol{x} - \boldsymbol{x}_k)$$

which now fits into (6b), or equivalently

$$-\|\boldsymbol{x}_k - \boldsymbol{a}_i\| - \partial\|\boldsymbol{x}_k - \boldsymbol{a}_i\|^T (\boldsymbol{x} - \boldsymbol{x}_k) + r_i - \delta_i \leq 0 \tag{3.14}$$

We remark that constraint (14) is not only convex but also tighter than (13b). As a matter of fact, the convexity of the norm $\|\boldsymbol{x} - \boldsymbol{a}_i\|$ implies that it obeys the property

$$\|\boldsymbol{x} - \boldsymbol{a}_i\| \geq \|\boldsymbol{x}_k - \boldsymbol{a}_i\| + \partial\|\boldsymbol{x}_k - \boldsymbol{a}_i\|^T (\boldsymbol{x} - \boldsymbol{x}_k)$$

Therefore, a point $\boldsymbol{x}$ satisfying (14) automatically satisfies (13b). Summarizing, the convexified problem in the k-th iteration can be stated as

$$\begin{aligned} \underset{\boldsymbol{x}}{\text{minimize}} \quad & \boldsymbol{x}^T\boldsymbol{x} - 2\boldsymbol{x}^T\boldsymbol{v}_k && \text{(3.15a)} \\ \text{subject to:} \quad & \|\boldsymbol{x} - \boldsymbol{a}_i\| - r_i - \delta_i \leq 0 && \text{(3.15b)} \end{aligned}$$

$$-\|\boldsymbol{x}_k - \boldsymbol{a}_i\| - \partial\|\boldsymbol{x}_k - \boldsymbol{a}_i\|^T (\boldsymbol{x} - \boldsymbol{x}_k) + r_i - \delta_i \leq 0 \tag{3.15c}$$

A technical problem making the formulation in (15) difficult to implement is that it requires a feasible initial point $\boldsymbol{x}_0$. The problem can be overcome by introducing nonnegative slack variables $s_i \geq 0, \hat{s}_i \geq 0$, for $i = 1, \ldots, m$ into the constraints in (15b) and (15c) to replace their right-hand sides (which are zeros) by relaxed upper bounds (as these new bounds themselves are nonnegative variables). This leads to a

penalty CCP (PCCP) based formulation as follows:

$$\underset{\boldsymbol{x},\boldsymbol{s},\hat{\boldsymbol{s}}}{\text{minimize}} \quad \boldsymbol{x}^T\boldsymbol{x} - 2\boldsymbol{x}^T\boldsymbol{v}_k + \tau_k \sum_{i=1}^{m}(s_i + \hat{s}_i) \tag{3.16a}$$

$$\text{subject to:} \quad \|\boldsymbol{x} - \boldsymbol{a}_i\| - r_i - \delta_i \leq s_i \tag{3.16b}$$

$$-\|\boldsymbol{x}_k - \boldsymbol{a}_i\| - \frac{(\boldsymbol{x}_k - \boldsymbol{a}_i)^T}{\|\boldsymbol{x}_k - \boldsymbol{a}_i\|}(\boldsymbol{x} - \boldsymbol{x}_k) + r_i - \delta_i \leq \hat{s}_i \tag{3.16c}$$

$$s_i \geq 0, \hat{s}_i \geq 0, \text{ for: } i = 1, 2, \ldots, m \tag{3.16d}$$

where the weight $\tau_k \geq 0$ increases as iterations proceed until it reaches an upper limit τ_{max}. By using a monotonically increasing τ_k for the penalty term in (16a), the algorithm reduces the slack variables s_i and $\hat{s}_i$ very quickly. As a result, new iterates quickly become feasible as s_i and $\hat{s}_i$ vanish. The upper limit τ_{max} is imposed to avoid numerical difficulties that may occur if τ_k becomes too large and to ensure convergence if a feasible region is not found [9]. Consequently, while formulation (16) accepts *infeasible* initial points, the iterates obtained by solving (16) are practically identical to those obtained by solving (15).

3.2.4 The Algorithm

The input parameters for the algorithm include the bound δ_i on the measurement error. Setting δ_i to a lower value leads to a "tighter" solution. On the other hand, a larger δ_i would make the algorithm less sensitive to outliers. If measurement noise $\boldsymbol{\varepsilon}$ obeys a Gaussian distribution with zero mean and known covariance $\boldsymbol{\Sigma} = \text{diag}(\sigma_1^2, \ldots, \sigma_m^2)$, then δ_i can be expressed as $\delta_i = \gamma\sigma_i$, where γ is a parameter that determines the width of confidence interval. For example, for $\gamma = 3$ we have the probability $Pr\{|\varepsilon_i| \leq 3\sigma_i\} \approx 0.99$. Other input parameters are initial point $\boldsymbol{x}_0$, maximum number of iterations K_{max}, initial weight τ_0, and upper limit of weight τ_{max} (to avoid numerical problems that may occur if τ_i becomes too large).

As mentioned in Sec. 2, the original LS objective is highly non-convex with many local minimums even for small-scale systems. Consequently, it is of critical importance to select a good initial point for the proposed PCCP-based algorithm because PCCP is essentially a local procedure. Several techniques are available, these include: (i) Select the initial point uniformly randomly over the same region as the unknown radiating source; (ii) Set the initial point to the origin; (iii) Run the algorithm from

a set of candidate initial points and identify the solution as the one with lowest LS error. Typically, comparing the results from n distinct initial points shall suffice. For the planar case ($n = 2$), for example, it is sufficient to compare the two intersection points of the two circles that are associated with the two smallest distance readings as the target is very likely to be in the vicinity of these sensors; and (iv) Apply a global localization algorithm such as those in [15] to generate an approximate LS solution, then take it as the initial point to run the proposed algorithm. The algorithm can be now outlined as follows.

PCCP-based LS Algorithm for Source Localization

Step 1: Input sensor locations $\{\boldsymbol{a}_i, i = 1, \ldots, m\}$, range measurements $\{r_i, i = 1, \ldots, m\}$, $\boldsymbol{x}_0, K_{max}, \tau_0, \tau_{max}, \mu > 0, \gamma, \sigma$, and set $k = 0$.

Step 2: Form $\boldsymbol{v}_k$ as in (10) and solve (16). Denote the solution as $(\boldsymbol{s}^*, \hat{\boldsymbol{s}}^*, \boldsymbol{x}^*)$.

Step 3: Update $\tau_{k+1} = \min(\mu\tau_k, \tau_{max})$, set $k = k + 1$.

Step 4: If $k = K_{max}$, terminate and output $\boldsymbol{x}^*$ as the solution; otherwise, set $\boldsymbol{x}_k = \boldsymbol{x}^*$ and repeat from Step 2.

3.3 Numerical Results

For illustration purposes, the proposed algorithm was applied to a network with five sensors, and its performance was evaluated and compared with existing state-of-the-art methods by Monte Carlo simulations with a set-up similar to that of [**?**]. SR-LS solutions were used as performance benchmarks for the PCCP-based LS Algorithm. The system consisted of 5 sensors $\{\boldsymbol{a}_i, i = 1, 2, \ldots, 5\}$ randomly placed in the planar region in $[-15; 15] \times [-15; 15]$, and a radiating source $\boldsymbol{x}_s$, located randomly in the region $\{\boldsymbol{x} = [x_1; x_2], -10 \leq x_1, x_2 \leq 10\}$. The coordinates of the source and sensors were generated for each dimension following a uniform distribution. Measurement noise $\{\varepsilon_i, i = 1, \ldots, m\}$ was modelled as independent and identically distributed (i.i.d) random variables with zero mean and variance σ^2, with σ being one of four possible levels $\{10^{-3}, 10^{-2}, 10^{-1}, 1\}$. The range measurements $\{r_i, i = 1, 2, \ldots, 5\}$ were calculated using (1). Accuracy of source location estimation was evaluated in terms of average of the squared position error error in the form $\|\boldsymbol{x}^* - \boldsymbol{x}_s\|^2$, where $\boldsymbol{x}_s$ denotes the exact source location and $\boldsymbol{x}^*$ is its estimation obtained by SR-LS and PCCP methods, respectively. In our simulations parameter γ was set to 3 and the number of iterations was set to 20. The proposed method was implemented by using CVX

Table 3.1: Averaged MSE for SR-LS and PCCP methods

σ	MLE	SR - LS	PCCP	R.I.
1e-03	6.0159e-01	1.3394e-06	**9.5243e-07**	29%
1e-02	3.5077e-01	1.4516e-04	**9.5831e-05**	34%
1e-01	3.7866e-01	1.2058e-02	**8.7107e-03**	28%
1e+0	1.4470e+00	1.3662e+00	**1.2346e+00**	10%

[36] and implementation of SR-LS followed [**?**]. The PCCP algorithm was initialized with intersection points of the two circles that are associated with the two smallest distance readings. A candidate solution point with lowest LS error in (2) was chosen as a PCCP solution. In cases when the circles did not intersect due to high noise level, the initial point was set as a midpoint between the centers of the two circles.

Table 3.1 provides comparisons of the PCCP with SR-LS and MLE, where each entry is averaged squared error over 1,000 Monte Carlo runs of the method. The MLE was implemented using Matlab function *lsqnonlin* [37], initialized with the same point as PCCP. It is observed that, comparing with SR-LS, the estimates produced by the proposed algorithm are found to be closer to the true source locations in MSE sense. The last column of the table represents relative improvement of the proposed method over SR-LS solutions in percentage.

Bibliography

[1] J. O. Smith and J. S. Abel, "Closed-form least-squares source location estimation from range-difference measurements," *IEEE Trans. on Acoustic, Speech Signal Proc.*, vol. 12, pp. 1661–1669, Dec. 1987.

[2] H. Schau and A. Robinson, "Passive source localization employing intersecting spherical surfaces from time-of-arrival differences," *IEEE Trans. on Acoustic, Speech Signal Proc.*, vol. ASSP–35, pp. 1223–1225, Aug. 1987.

[3] K. Yao, R. Hudson, C. Reed, D. Chen, and F. Lorenzelli, "Blind beamforming on a randomly distributed sensor array system," *IEEE J. Select. Areas Commun.*, vol. 16, pp. 1555-1567, Oct. 1998.

[4] M. A. Sprito, "On the accuracy of cellular mobile station location estimation," *IEEE Trans. on Veh. Technol.*, vol. 50, pp. 674-685, May 2001.

[5] Y. Huang, J. Benesty, G. W. Elko, and R. M. Mersereau, "Realtime passive source localization: A practical linear correction least-squares approach," *IEEE Trans. on Speech Audio Proc.*, vol. 9, no. 8, pp. 943-956, Nov. 2002.

[6] K. W. Cheung, H. C. So, W. K. Ma, and Y. T. Chan, "Least squares algorithms for time-of-arrival-based mobile location," *IEEE Trans. on Signal Proc.*, vol. 52, no. 4, pp. 1121–1228, Apr. 2004.

[7] D. Li and H. Hu, "Energy-Based Collaborative Source Localization Using Acoustic Microsensor Array," in *EURASIP Journal on Applied Signal Proc.*, vol. 4, 321–337, 2003.

[8] X. Sheng and Y.-H. Hu, "ML Multiple-source localization using acoustic energy measurements with wireless sensor networks," *IEEE Trans. on Signal Proc.*, vol. 53, no.1, pp. 44–53, Jan. 2005.

[9] Z. M. Saric, D. D. Kukolj, and N. D. Teslic, "Acoustic source localization in wireless sensor network", *Circuits Syst Signal Proc.*, vol. 29, pp. 837–856, 2010.

[10] L.Lu, H.-C. Wu, K.Yan, and S.Iyengar, "Robust expectation maximization algorithm for multiple wideband acoustic source localization in the presence of nonuniform noise variances," *IEEE Sensors J.*, vol. 11, no. 3, pp. 536544, Mar. 2011

[11] K.W. Cheung, W.K. Ma, and H.C. So, "Accurate approximation algorithm for TOA-based maximum-likelihood mobile location using semidefinite programming," in *Proc. ICASSP*, vol. 2, pp. 145–148, 2004.

[12] A. H. Sayed, A. Tarighat, and N. Khajehnouri, "Network-based wireless location," *IEEE Signal Pro. Mag.*, vol. 22, no. 4, pp. 24–40, July 2005.

[13] Y. T. Chan, H. Y. C. Hang, and P. C. Ching, "Exact and approximate maximum likelihood localization algorithms," *IEEE Trans. on Veh. Technol.*, vol. 55, no. 1, pp. 10–16, Jan. 2006.

[14] P. Stoica and J. Li, "Source localization from range-difference measurements," *IEEE Signal Proc. Mag.*, vol. 23, pp. 63–65,69, Nov. 2006.

[15] A. Beck, P. Stoica and J. Li, "Exact and approximate solutions of source localization problems," *IEEE Trans. on Signal Proc.*, vol. 56, no. 5, pp. 1770–1777, May 2008.

[16] A. Beck, M. Teboulle, and Z. Chikishev, "Iterative minimization schemes for solving the single source localization problem," *SIAM J. Optim.*, vol. 19, no. 3, pp. 1397–1416, Nov. 2008.

[17] I. Daubechies, R. DeVore, M. Fornasier, and C. S. Güntürk, "Iteratively reweighted least squares minimization for sparse recovery," *Comm. Pure Appl. Math.*, vol. 63, pp. 1–38, 2010.

[18] A. Beck, and D. Pan, "On the solution of the GPS localization and circle fitting problems," *SIAM J. Optim.*, vol. 22, no. 1, pp. 108–134, Jan. 2012.

[19] A. Beck, "On the convergence of alternating minimization for convex programming with applications to iteratively re-weighted least squares and decomposition schemes," *SIAM J. Optim.*, vol. 25, no. 1, pp. 185-209, Jan. 2015.

[20] J.J. More, "Generalizations of the trust region subproblem," *Optim. Methods Softw.*, vol. 2, pp. 189–209, 1993.

[21] C. Fortin and H. Wolkowicz, "The trust region subproblem and semidefinite programming," *Optim. Methods Softw.*, vol. 19, no.1, pp. 41–67, 2004.

[22] D.P. O'Leary, "Robust regression computation using iteratively reweighted least squares," *SIAM J. Matrix Anal. Appl.*, vol. 11, no. 3, pp. 466–480, 1990.

[23] N. Bissantz, L. Dümbgen, A. Munk, and B. Stratmann, "Convergence analysis of generalized iteratively reweighted least squares algorithms on convex function spaces," *SIAM J. Optim.*, vol. 19, no. 4, pp 1828–1845, 2009.

[24] K. W. Cheung and H. C. So, "A multidimensional scaling framework for mobile location using time-of-arrival measurements," *IEEE Trans. on Signal Proc.*, vol. 53, no. 2, pp. 460–470, Feb. 2005.

[25] H. Liu, H. Darabi, P. B, and J. Liu, "Survey of Wireless Indoor Positioning Techniques and Systems," *IEEE Trans. on Systems, Man and Cybernetics. Part C: Applications and Revies*, vol. 37, no. 6, pp. 1067–1080 ,Nov. 2007

[26] Y. Liu, Y.H. Hu, and Q. Pan, "Distributed, Robust Acoustic Source Localization in a Wireless Sensor Network," *IEEE Trans. on Signal Proc.*, vol. 60, no. 8, pp. 4350–4359, Aug. 2012.

[27] W. Kim, J. Lee, and G. Jee, "The interior-point method for an optimal treatment of bias in trilateration location," *IEEE Trans. Veh. Technol.*, vol. 55, no. 4, pp. 12911301, Jul. 2006.

[28] T. Qiao, S. Redfield, A. Abbasi, Z. Su, and H. Liu, "Robust coarse position estimation for TDOA localization," *IEEE Wireless Commun. Lett.*, vol. 2, no. 6, pp. 623626, Dec. 2013.

[29] A. L. Yuille and A. Rangarajan, "The concave-convex procedure,' *Neural Computation*, vol. 15, no. 4, pp. 915–936, 2003.

[30] T. Lipp and S. Boyd, "Variations and extensions of the convex-concave procedure," *Research Report*, Stanford University, Aug. 2014.

[31] G. R. Lanckreit and B. K. Sriperumbudur, "On the convergence of the concave-convex procedure," in *Advances in Neural Information Proc. Systems*, pp. 1759–1767, 2009.

[32] L. Vandenberghe and S. Boyd, "Semidefinite programming," *SIAM Rev.*, vol. 38, no. 1, pp. 40–95, Mar. 1996.

[33] A. Antoniou and W.-S. Lu, *Practical Optimization: Algorithms and Engineering Applications*, Springer, 2007.

[34] Y. Nesterov, *Introductory Lectures on Convex Optimization*, Kluwer, 2004.

[35] *Geolocation Techniques*

[36] CVX Research, http://cvx.com/cvx, August 2012.

[37] The Mathworks Inc., http://mathworks.com, 2015.